

Redox-Controllable Amphiphilic [2]Rotaxanes

Hsian-Rong Tseng,^[a] Scott A. Vignon,^[a] Paul C. Celestre,^[a] Julie Perkins,^[a]
Jan O. Jeppesen,^[b] Alberto Di Fabio,^[c] Roberto Ballardini,^[d] M. Teresa Gandolfi,^{*,[c]}
Margherita Venturi,^{*,[c]} Vincenzo Balzani,^[c] and J. Fraser Stoddart^{*,[a]}

Abstract: With the fabrication of molecular electronic devices (MEDs) and the construction of nanoelectromechanical systems (NEMSs) as incentives, two constitutionally isomeric, redox-controllable [2]rotaxanes have been synthesized and characterized in solution. Therein, they both behave as near-perfect molecular switches, that is, to all intents and purposes, these two rotaxanes can be switched precisely by applying appropriate redox stimuli between two distinct chemomechanical states. Their dumbbell-shaped components are composed of polyether chains interrupted along their lengths by i) two π -electron rich recognition sites—a tetrathiafulvalene (TTF) unit and a 1,5-dioxynaphthalene (DNP) moiety—with ii) a rigid terphenylene spacer placed between the two recognition sites, and then terminated by iii) a hydrophobic tetraarylmethane stopper at one end and a hydrophilic dendritic stopper at the other end of the dumbbells, thus conferring amphiphilicity upon these molecules. A template-directed protocol produces a means to introduce the tetracationic cyclophane, cyclobis(paraquat-*p*-phenylene) (CBPQT⁴⁺), which contains two π -electron accepting bipyridinium units,

mechanically interlocked around the dumbbell-shaped components. Both the TTF unit and the DNP moiety are potential stations for CBPQT⁴⁺, since they can establish charge-transfer and hydrogen bonding interactions with the bipyridinium units of the cyclophane, thereby introducing bistability into the [2]rotaxanes. In both constitutional isomers, ¹H NMR and absorption spectroscopies, together with electrochemical investigations, reveal that the CBPQT⁴⁺ ring is predominantly located on the TTF unit, leading to the existence of a single translational isomer (co-conformation) in both cases. In addition, a model [2]rotaxane, incorporating hydrophobic tetraarylmethane stoppers at both ends of its dumbbell-shaped component, has also been synthesized as a point of reference. Molecular synthetic approaches were used to construct convergently the dumbbell-shaped compounds by assembling progressively smaller building blocks in

the shape of the rigid spacer, the TTF unit and the DNP moiety, and the hydrophobic and hydrophilic stoppers. The two amphiphilic bistable [2]rotaxanes are constitutional isomers in the sense that, in one constitution, the TTF unit is adjacent to the hydrophobic stopper, whereas in the other, it is next to the hydrophilic stopper. All three bistable [2]rotaxanes have been isolated as green solids. Electrospray and fast atom bombardment mass spectra support the gross structural assignments given to all three of these mechanically interlocked compounds. Their photophysical and electrochemical properties have been investigated in acetonitrile. The results obtained from these investigations confirm that, in all three [2]rotaxanes, i) the CBPQT⁴⁺ cyclophane encircles the TTF unit, ii) the CBPQT⁴⁺ cyclophane shuttles between the TTF and DNP stations upon electrochemical or chemical oxidation/reduction of the TTF unit, and iii) folded conformations are present in which the CBPQT⁴⁺ cyclophane, while encircling the TTF unit, interacts through its π -accepting bipyridinium exteriors with other π -donating components of the dumbbells, especially those located within the stoppers.

Keywords: molecular shuttle · nanoscale switches · redox processes · self-assembly · template-directed synthesis · tetrathiafulvalene

[a] Dr. H.-R. Tseng, S. A. Vignon, P. C. Celestre, Dr. J. Perkins,
Prof. Dr. J. F. Stoddart
Department of Chemistry and Biochemistry
University of California, Los Angeles
405 Hilgard Avenue, Los Angeles, CA 90095-1569 (USA)
Fax: (+1) 310-206-1843
E-mail: stoddart@chem.ucla.edu

[b] Dr. J. O. Jeppesen
Department of Chemistry
Odense University (University of Southern Denmark)
Campusvej 55, 5230, Odense M (Denmark)

Fax: (+45) 66-15-87-80
E-mail: joj@chem.sdu.dk

[c] A. Di Fabio, Prof. M. T. Gandolfi, Prof. M. Venturi, Prof. V. Balzani
Dipartimento di Chimica "G. Ciamician"
Università di Bologna
Via Selmi 2, 40126 Bologna (Italy)
Fax: (+39) 051-209-9456
E-mail: vbalzani@ciam.unibo.it

[d] Dr. R. Ballardini
Ist. ISOF-CNR, Via Gobetti 101
40129 Bologna (Italy)

Introduction

Supramolecular chemistry^[1] and self-assembly^[2] have emerged as a powerful vehicle and key concept, respectively, for the development of synthetic chemistry^[3] to a point where making rotaxanes using template-directed protocols^[4] is now routine. A [2]rotaxane is a molecule composed of a ring and a dumbbell-shaped component.^[5] The ring component encircles the linear, rod-like portion of the dumbbell-shaped component and is trapped mechanically by two bulky stoppers. If two identical recognition sites for the ring component are located within the dumbbell-shaped component, then the outcome is a degenerate equilibrium state in which the ring shuttles back and forth along the linear portion of the dumbbell. Such a [2]rotaxane constitutes a molecular shuttle.^[6] When the two different recognition sites which are incorporated into the dumbbell component differ in their constitutions, then the [2]rotaxane can exist in two different equilibrating translational isomers^[7] or co-conformations;^[8] their populations reflect the relative free energies, as determined primarily by the strengths of the two different sets of noncovalent bonding interactions present in the mechanically interlocked molecules. Moreover, these molecules can be activated by switching the recognition sites on and off between the components chemically,^[9] electrochemically,^[10] electrically,^[11] and optically,^[12] such that their components perform relative motions—that is, overall, the [2]rotaxane behaves as a controllable molecular shuttle^[6] wherein the movement of the ring component can be induced by an appropriate stimulus to shuttle in a linear fashion between the two recognition sites. Since the ring and dumbbell-shaped components of these highly ordered interlocked molecules can be induced to perform these relative internal motions, rotaxanes are now prime candidates for the construction of artificial molecular machines,^[13,14] which, in the appropriate solid-state settings, become the blueprints for the fabrication^[11,15] of molecular electronic devices (MEDs) and the engineering of nanoelectromechanical systems (NEMSs).

Not so long ago, we described^[16] the template-directed syntheses^[4] of amphiphilic, bistable rotaxanes composed of dumbbell-shaped components with two recognition sites—namely a monopyrrolo-tetrathiafulvalene (MP-TTF) unit and a 1,5-dioxynaphthalene (DNP) moiety—and a common ring component, that is, cyclobis(paraquat-*p*-phenylene)^[17] (CBPQT⁴⁺). In the ideal switch, [π - π] stacking and other interactions^[18] involving the CBPQT⁴⁺ ring and the stronger (MP-TTF) of the two π -electron-donating recognition sites would result in these [2]rotaxanes existing as a single translational isomer with the CBPQT⁴⁺ ring encircling only the MP-TTF unit. In practice, however, electrochemical studies, supported by spectroscopic results, have shown^[16,19] that, in these particular rotaxanes, both translational isomers are present in approximately 1:1 ratios in Me₂CO solutions at room temperature. It follows that, if this equilibrium is the starting point, then oxidation of the MP-TTF units will only activate half of the molecules, that is, only 50% of them are available to undergo switching. This inherent lack of precise mechanical control compromises the performance of these

[2]rotaxanes when it comes to fabricating MEDs and engineering NEMSs.

In an attempt to produce [2]rotaxanes which will function as linear motor-molecules with 100% precision, we have elected to employ a simple disubstituted TTF unit in competition with the DNP moiety. Since we already knew that TTF forms a strong green 1:1 complex ($K_a = 10000\text{M}^{-1}$ in MeCN)^[6b,20] with CBPQT⁴⁺, whereas 1,5-dihydroxynaphthalene forms a much weaker red 1:1 complex ($K_a = 770\text{M}^{-1}$ in MeCN)^[21] with CBPQT⁴⁺, the idea seemed to be a potentially productive one. Moreover, a closely related non-degenerate [2]catenane, based on identical TTF and DNP recognition sites has been demonstrated to behave as a nearly perfect switch, both in solution^[22a,b] and in a solid-state device.^[22c]

In a recent preliminary communication,^[23] we have described i) the synthesis of the model [2]rotaxane **1**·4PF₆ in which the ring component is CBPQT⁴⁺ and the dumbbell-shaped component contains both TTF and DNP recognition sites, separated by a rigid terphenylene spacer and terminated by two hydrophobic tetraarylmethane stoppers, and ii) the characterization by UV/Vis and ¹H NMR spectroscopies of the “clean” redox switching action in solution of this bistable rotaxane, wherein a relative mechanical movement of several nanometers on the part of the CBPQT⁴⁺ ring occurs along the axis of the dumbbell, assuming the gross structure of its rod section to be linear, as portrayed in Figure 1.

In order to investigate the properties and characteristics of solid-state devices, based on this nearly perfect electro-mechanical switch, we have identified, as synthetic targets, two amphiphilic bistable [2]rotaxanes, **3**·4PF₆ and **5**·4PF₆ in which the ring component (CBPQT⁴⁺) and the rod section—containing TTF and DNP recognition sites separated by a terphenylene spacer—of the dumbbell-shaped component are retained but in which one of the two hydrophobic stoppers is replaced in turn by a hydrophilic dendritic one. It is clear from a perusal of Figure 1 that these two rotaxanes are constitutional isomers in the sense that, in **3**⁴⁺, the TTF unit encircled by the CBPQT⁴⁺ ring, is adjacent to the hydrophobic stopper, whereas, in **5**⁴⁺, it is next to the hydrophilic stopper. Although we would expect these two bistable rotaxanes, because of their amphiphilic character, to be largely elongated within Langmuir monolayers at the air-water interface, and in Langmuir-Blodgett (LB) films in device settings (Figure 1b and c), the fact that all three of these rotaxanes, namely **1**⁴⁺, **3**⁴⁺, and **5**⁴⁺, are relatively long and flexible means that quite a number of alongside intramolecular interactions involving the CBPQT⁴⁺ ring and the DNP moiety, as well as π -electron rich aromatic units present in the hydrophilic-dendritic and hydrophobic stoppers of **3**⁴⁺ and **5**⁴⁺, could lead to some rather contorted and exotic conformations^[10c,19,24] being populated in solution. It is important that the solution-state properties of these bistable amphiphilic [2]rotaxanes are understood at the same time as their performances in devices are being evaluated.

In this paper, we describe the template-directed synthesis of the three bistable [2]rotaxanes shown in Figure 1—namely i) the model rotaxane **1**·4PF₆ and ii) the two consti-

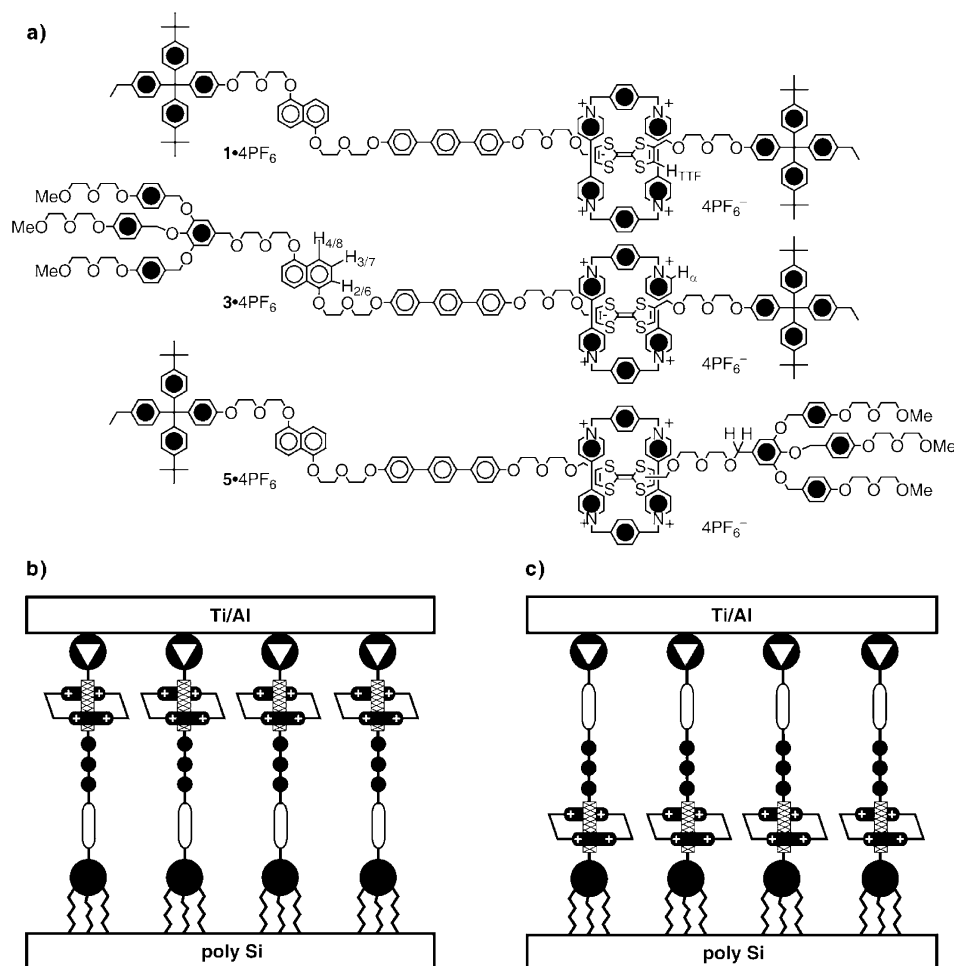


Figure 1. a) Structural formulas of the bistable [2]rotaxane **1•4PF₆** and amphiphilic bistable [2]rotaxanes **3•4PF₆** and **5•4PF₆**. b) and c) Idealized graphical representations of the two constitutional isomers **3⁺** and **5⁺**, respectively, in device settings between polysilicon and Ti/Al electrodes. The LB technique is used in the first place to self-organize these two amphiphilic bistable [2]rotaxanes.

tutional isomers **3•4PF₆** and **5•4PF₆**, prior to iii) presenting and discussing the results of mass spectrometry and ¹H NMR spectroscopic, photophysical, and electrochemical investigations carried out on all three [2]rotaxanes, as well as on the corresponding dumbbell compounds **2**, **4**, and **6** (Schemes 3–5) and their model compounds (Figure 2)—namely, **10**, **35**, CBPQT⁴⁺ (**36⁴⁺**), **37**,^[25] **38**,^[19] and **39**.^[26] The discussion is concluded by iv) presenting the results of redox-switching experiments carried out on all three bistable [2]rotaxanes.

Results and Discussion

Design and synthetic strategy:

Retrosynthetic analyses of the model [2]rotaxane **1•4PF₆** and

can be achieved efficiently with reasonably little effort. Moreover, the reactions, which were chosen (Schemes 1–5) for connecting each fragment, are nucleophilic substitutions

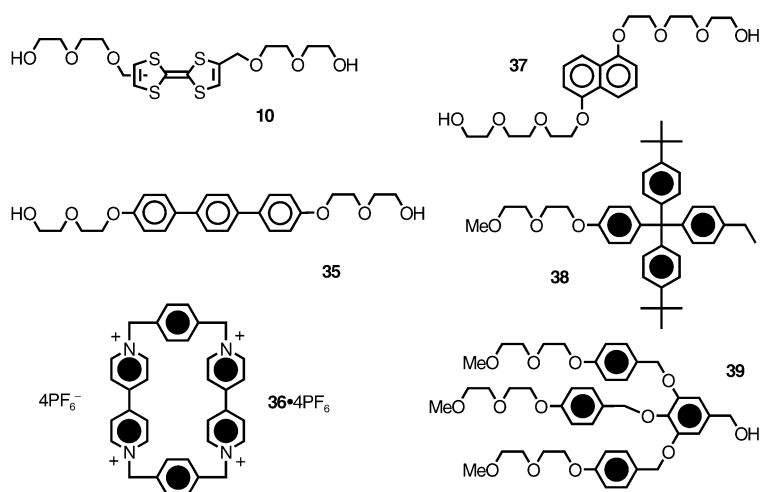
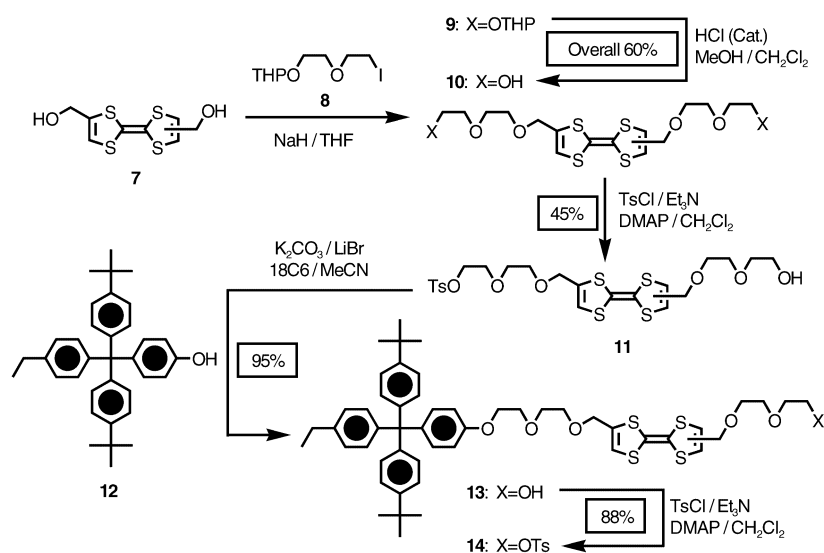


Figure 2. Structural formulas of the cyclophane **36•4PF₆**, and of the compounds used as models.

the amphiphilic [2]rotaxanes **3•4PF₆** and **5•4PF₆** revealed a considerable range of possible synthetic pathways. Common to all of these possible routes is the key clipping reaction to form the CBPQT⁴⁺ ring around the dumbbell-shaped compounds, a template-directed procedure which always constitutes the last step of the syntheses, which are presented in Schemes 1–5. In order to obtain the dumbbell compounds **2**, **4**, and **6** as conveniently as possible, a modular synthetic approach was adopted for the progressive assembly of the five different fragments—namely i) the hydrophobic tetraarylmethane stopper^[11c,27] **12** (Scheme 1), ii) the hydrophilic dendritic stopper^[11c,26] (Schemes 4 and 5), iii) the TTF building block **10**, (Scheme 1), iv) the DNP building block^[25] **24** (Scheme 4), and v) the terphenylene spacer which was introduced by first incorporating the biphenyl **16** into an intermediate compound, followed by coupling (Schemes 2 and 4) with the Grignard reagent **19**. Since all the synthetic pathways share these common intermediates, the syntheses of [2]rotaxanes **1•4PF₆**, **3•4PF₆**, and **5•4PF₆**

Scheme 1. Synthesis of the TTF containing half-dumbbell compound **14**.

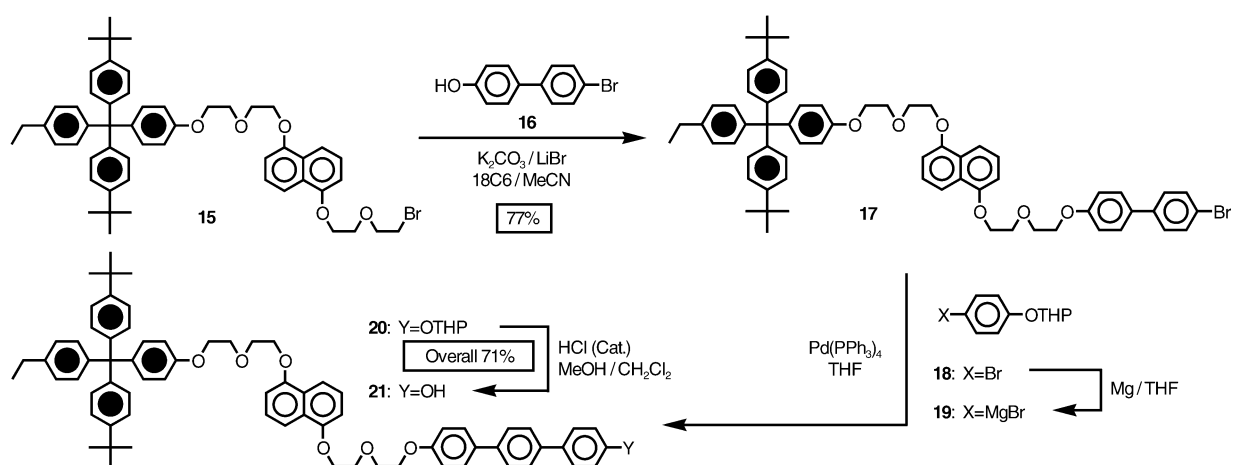
between the bromides or monotosylates and the appropriate alcohols in the presence of basic reagents and these reactions are usually high yielding and reproducible. Using this modular strategy, the model [2]rotaxane **1-4**PF₆, and the two amphiphilic [2]rotaxanes **3-4**PF₆ and **5-4**PF₆, were obtained (Schemes 1–5) with relative ease.

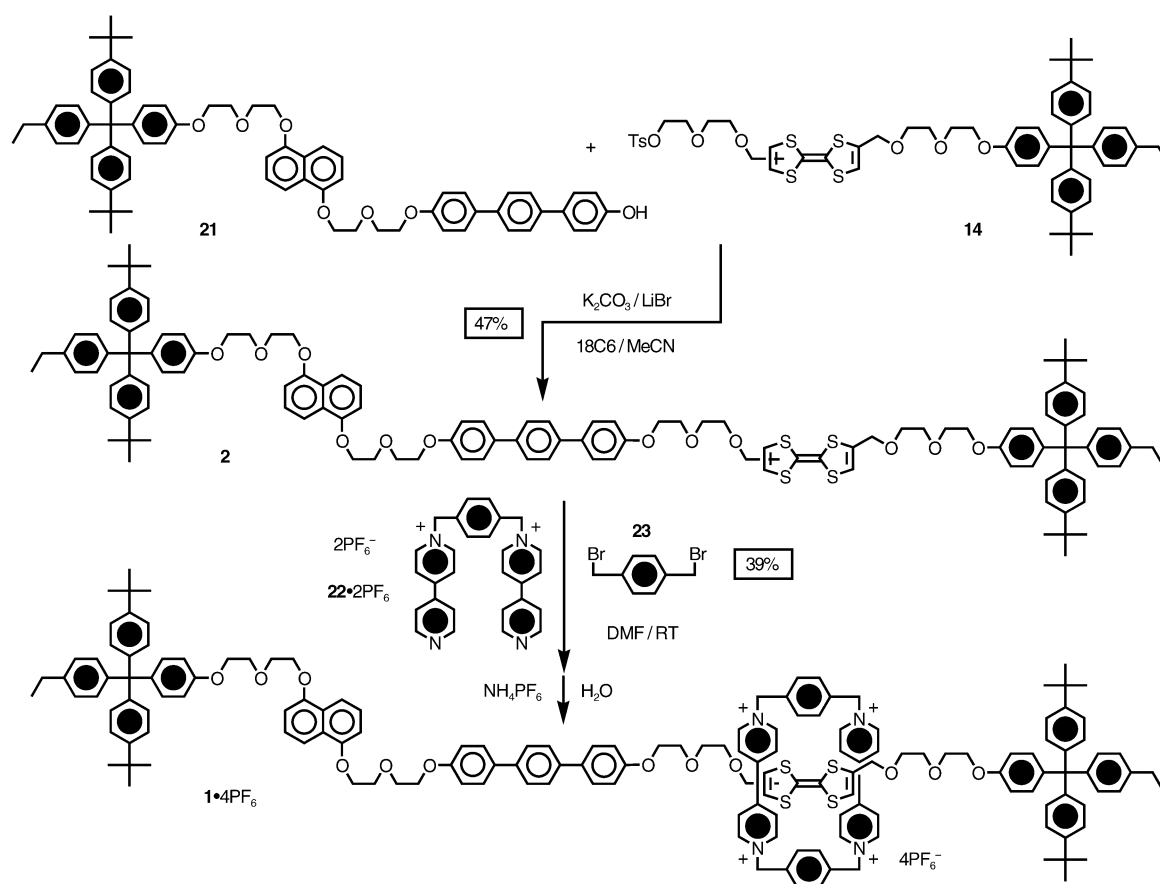
Synthesis: The route for the synthesis of the model [2]rotaxane **1-4**PF₆ is described in Schemes 1–3. The dumbbell-shaped compound **2** was obtained (Scheme 3) in 47% yield by alkylating the phenol **21** (produced in Scheme 2), with the tosylate **14** (produced in Scheme 1) using LiBr and [18]crown-6 as catalysts in the presence of K₂CO₃ as base. The preparation of the TTF-containing half-dumbbell compound **14** (Scheme 1) begins with alkylation of the diol^[28] **7** by the iodide^[29] **8** in THF using eight equivalents of NaH. Without purification, the resulting compound **9** was converted into the diol **10** by HCl-catalyzed deprotection in a MeOH/CH₂Cl₂ solvent mixture with an overall yield of 60% for the two steps. Subsequent tosylation of the diol **10** with

one equivalent of TsCl afforded the monotosylate **11** in 45% yield after flash column chromatography. The high yielding (95%) alkylation of the phenolic tetraarylmethane stopper^[11c, 27] **12** with the monotosylate **11** was achieved in MeCN with LiBr and [18]crown-6 as catalysts in the presence of K₂CO₃ as base. Tosylation of the resulting alcohol **13** gave the tosylate **14** in 88% yield. The preparation of the DNP-containing half-dumbbell-shaped compound **21** is outlined in Scheme 2. Using conventional alkylation conditions (K₂CO₃/LiBr/[18]crown-6/MeCN), 4-bromo-(1,1'-biphenyl)-4-ol (**16**) was treated with the bromide^{[16,}

^{19]} **15** to give compound **17** in 77% yield. The synthesis of the terphenylene compound **20** was accomplished by means of a Pd⁰-catalyzed cross-coupling reaction in THF with the freshly prepared Grignard reagent **19** from the THP-ether **18** of *p*-bromophenol. HCl-Catalyzed deprotection of compound **20** gave the phenol **21** in 71% yield overall. The [2]rotaxane **1-4**PF₆ was obtained (Scheme 3) by a template-directed synthesis, using the dumbbell compound **2** as a template, to form a CBPQT⁴⁺ ring from its dicationic precursor^[30] **22-2**PF₆ and α,α' -dibromoxylene (**23**). The [2]rotaxane **1-4**PF₆ was isolated in 39% yield as an analytically pure green solid after chromatography on silica gel using a 1% NH₄PF₆ solution in Me₂CO as the eluent.

The sequence of steps employed in the synthesis of the rotaxane **3-4**PF₆ and its precursor dumbbell compound **4** is summarized in Scheme 4. The monobromination of the diol^[25] **24** with CBr₄ and PPh₃ afforded in 35% yield the bromide **25** which was subsequently treated with TBDMSCl to obtain the silyl ether **26** in quantitative yield. Alkylation of **26** with 4-bromo-(1,1'-biphenyl)-4-ol (**16**) gave compound

Scheme 2. Synthesis of the DNP containing half-dumbbell compound **21**.

Scheme 3. Synthesis of the bistable [2]rotaxane $1\cdot 4\text{PF}_6$.

27 in 62% yield. The synthesis of the terphenylene derivative **28** was accomplished by the cross-coupling reaction between **27** and the freshly prepared Grignard reagent **19** in the presence of $[\text{Pd}(\text{PPh}_3)_4]$. TFA-Catalyzed deprotection of **28** gave the phenol **29** in 71% yield overall. The TTF-DNP-containing half-dumbbell **30** was obtained in 82% yield by carrying out an alkylation between phenol **29** and tosylate **14** with K_2CO_3 as base in MeCN. In the presence of NaH, the half-dumbbell compound **30** was treated with the dendritic chloride^[11c,26] **31** with NaI and [15]crown-5 as catalysts to afford the dumbbell compound **4** in 51% yield. The template-directed synthesis of the [2]rotaxane $3\cdot 4\text{PF}_6$ proceeded in 60% yield when the reaction of the dumbbell compound **4**, the dicationic salt $22\cdot 2\text{PF}_6$ and dibromide **23**, using exactly the same reaction and isolation conditions of those employed in the preparation of $1\cdot 4\text{PF}_6$, was carried out.

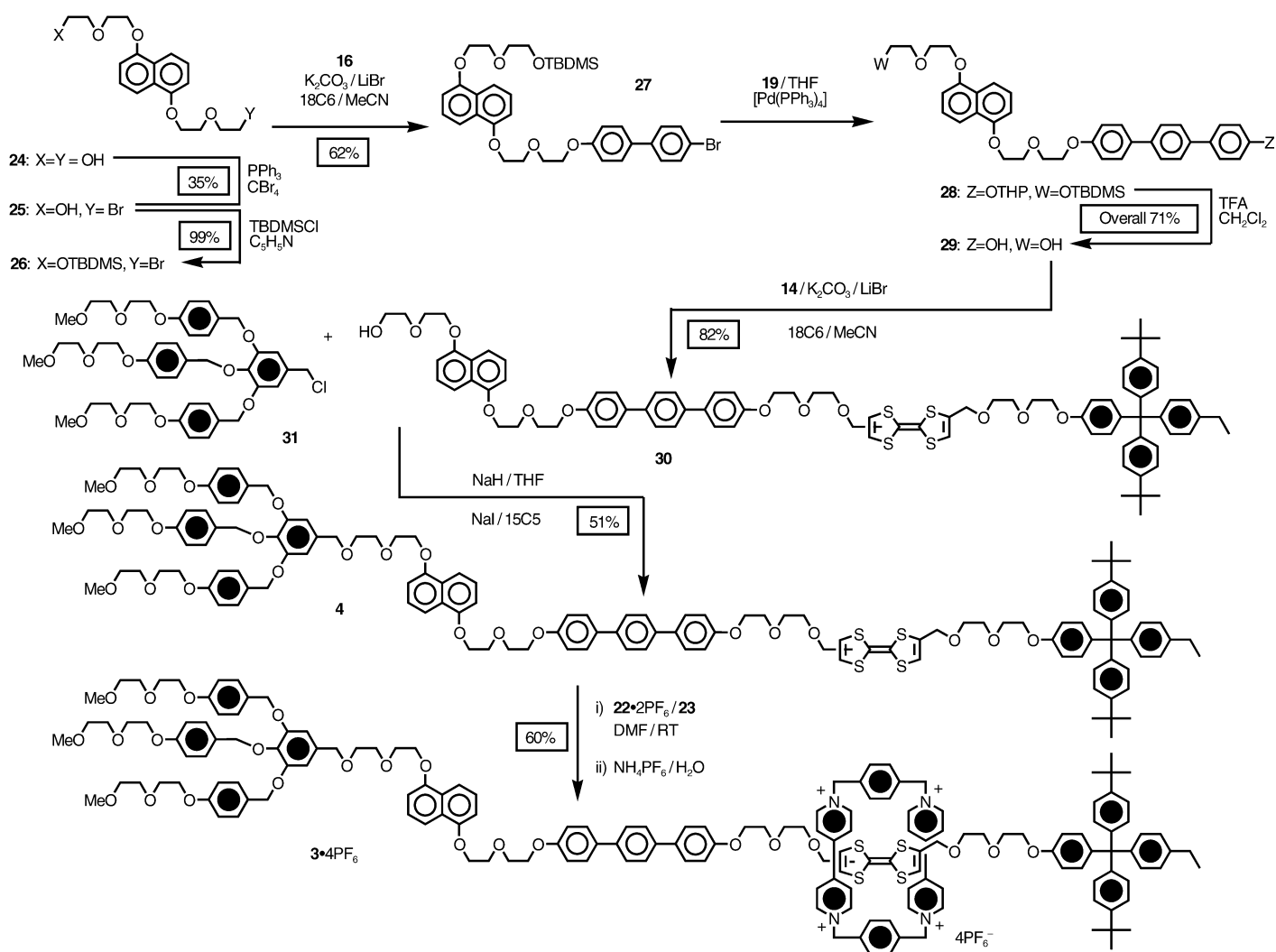
The template-directed synthesis of the rotaxane $5\cdot 4\text{PF}_6$ from its dumbbell-shaped precursor **6** is summarized in Scheme 5. The half-dumbbell **32** was obtained in 64% yield from a substitution reaction ($\text{K}_2\text{CO}_3/\text{LiBr}/[18]\text{crown-6}/\text{MeCN}$) carried out between monotosylate **11** and phenol **21**. The dendritic chloride^[11c,26] **31** and the half-dumbbell **32** were treated in the presence of NaH, NaI and [15]crown-5 to afford the dumbbell compound **6** in 66% yield. Once again, the template-directed synthesis of the [2]rotaxane $5\cdot 4\text{PF}_6$ was achieved, this time in 57% yield from the dumb-

bell compound **6**, using the protocol already described for making $3\cdot 4\text{PF}_6$.

The model compound **35** was synthesized (Scheme 6) by alkylation of the diol^[31] **33** with the chloride **34** in DMF in the presence of K_2CO_3 and LiBr.

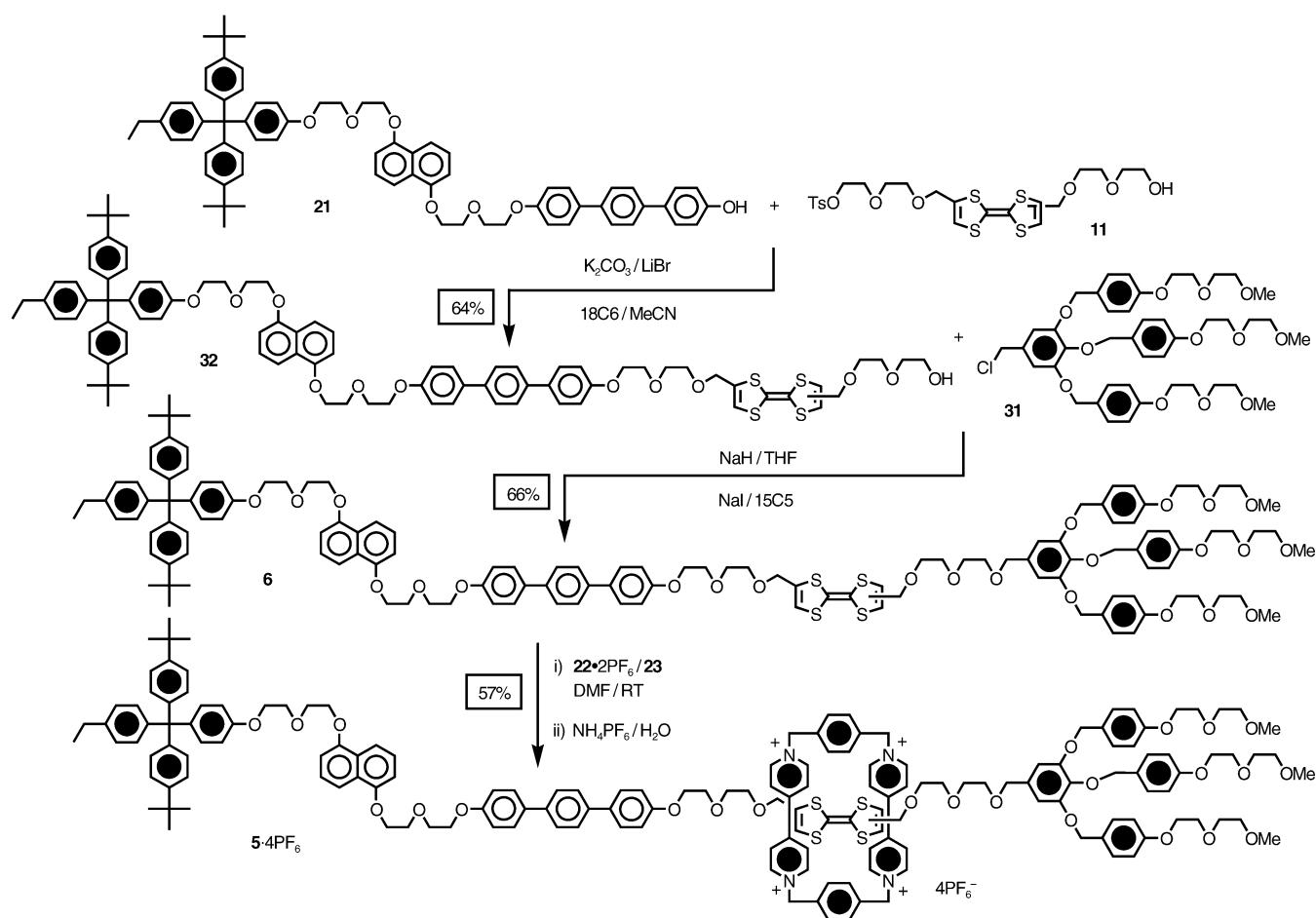
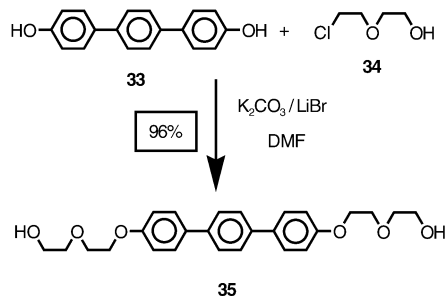
Mass spectrometric investigation: Mass spectral data for the [2]rotaxanes $1\cdot 4\text{PF}_6$, $3\cdot 4\text{PF}_6$, and $5\cdot 4\text{PF}_6$ are summarized in Table 1. The model [2]rotaxane $1\cdot 4\text{PF}_6$ was characterized by electrospray (ES) mass spectrometry. The ES mass spectrum of $1\cdot 4\text{PF}_6$ revealed five peaks which correspond to the doubly positively-charged ions $[M-2\text{PF}_6]^{2+}$ and $[M-3\text{PF}_6]^{2+}$, the triply positively-charged ion $[M-3\text{PF}_6]^{3+}$, and the quadruply positively-charged ion $[M-4\text{PF}_6]^{4+}$. The amphiphilic [2]rotaxanes $3\cdot 4\text{PF}_6$ and $5\cdot 4\text{PF}_6$ were characterized by fast atom bombardment (FAB) mass spectrometry. In both cases, six major peaks, corresponding to the singly positively-charged ions $[M-2\text{PF}_6]^+$, $[M-2\text{PF}_6]^+$, and $[M-3\text{PF}_6]^+$ and doubly positively charged ions $[M-2\text{PF}_6]^{2+}$, $[M-3\text{PF}_6]^{2+}$, and $[M-4\text{PF}_6]^{2+}$, were observed in their FAB mass spectra.

^1H NMR Spectroscopic investigation: Only one translational isomer—the one in which the CBPQT⁴⁺ ring encircles the TTF unit—is indicated by ^1H NMR spectroscopy to be present in the intensely green CD_3CN solutions of each of the three [2]rotaxanes $1\cdot 4\text{PF}_6$, $3\cdot 4\text{PF}_6$, and $5\cdot 4\text{PF}_6$ recorded at

Scheme 4. Synthesis of the amphiphilic, bistable [2]rotaxane **3·4PF₆**.

room temperature. The ¹H NMR spectra (Figure 3) of all three of these compounds in CD₃CN at 500 MHz exhibit a highly characteristic signature—that is, in each case, two pairs of signals of unequal intensities resonating at δ 5.98, 6.06, 6.17, and 6.23 for **1·4PF₆** (Figure 3a), at δ 5.96, 6.06, 6.16, and 6.22 for **3·4PF₆** (Figure 3b), and at δ 5.92, 5.98, 6.10, and 6.20 for **5·4PF₆** (Figure 3c)—for the constitutionally heterotopic methine protons on the CBPQT⁴⁺-encircled TTF units with equilibrating (slow on the ¹H NMR time-scale but fast on the isolation one) pairs of *cis* and *trans* isomers as a result of torsion about the formal double bond in the midst of the disubstituted TTF units. So far, we have not been able to assign the two pairs of singlets of unequal intensities to the *cis* and *trans* isomers, but we believe they are the only two species that are significantly populated in solutions of **1⁴⁺**, **3⁴⁺**, and **5⁴⁺** as their 4PF₆[−] salts. Variable temperature ¹H NMR experiments were performed on all three compounds in both CD₃CN and CD₃COCD₃ over 170° ranges between 190 and 360 K. No temperature dependent behavior was observed that might be indicative of more than one translational isomer existing in solutions of these [2]rotaxanes. They do, however, exist as a mixture of major

and minor isomers in relation to the *cis-trans* configurations associated with the CBPQT⁴⁺-encircled TTF units in **1⁴⁺**, **3⁴⁺**, and **5⁴⁺**. Incontrovertible evidence for the presence in these three rotaxanes of folded conformations, wherein π-donating residues in the dumbbell components associate themselves with the π-accepting bipyridinium exteriors of the CBPQT⁴⁺ rings, will be presented subsequently in the subsections (see below) of this Results and Discussion section on photophysical and electrochemical investigations. We just wish to make the point here that there is some circumstantial evidence, from a comparison (Table 2 and Figure 3) of the ¹H NMR spectra of the three rotaxanes, not only for the existence of such folded conformations, but also for their different proportions, and possibly structures as well. Parts a), b), and c) of Figure 3 show, respectively, the ¹H NMR spectra of the rotaxanes **1⁴⁺**, **3⁴⁺**, and **5⁴⁺** recorded in CD₃CN at room temperature. Disregarding the peaks in the spectrum (Figure 3b) for **3⁴⁺** that result from the portions in the hydrophilic stopper, it is evident from close inspections of the relevant spectra (Figure 3a and b) that rotaxane **1⁴⁺** and **3⁴⁺** display a very similar array of signals. By contrast, the spectrum (Figure 3c) for the rotaxane **5⁴⁺** is

Scheme 5. Synthesis of the amphiphilic, bistable [2]rotaxane $5\cdot 4\text{PF}_6$.Scheme 6. Synthesis of the terphenyl compound **35**.

significantly different from those (Figure 3a and b) of the other two. This point is further emphasized by the chemical shift data presented in Table 2 for selected proton probes in the three rotaxanes. The δ values shown in italics for $5\cdot 4\text{PF}_6$, differ significantly from those for $1\cdot 4\text{PF}_6$ and $3\cdot 4\text{PF}_6$, which are themselves very similar, one with the other. These

observations anticipate the more detailed analysis (see below), based on electrochemical data, wherein 1^{4+} and 3^{4+} are found to behave quite similarly, while 5^{4+} is the odd one out. It should be noted that the ^1H NMR spectroscopic data is concentration independent, an observation which rules out intermolecular aggregation as a significant contribution to the overall picture.^[32]

Photophysical investigations: The photophysical properties were studied in air-equilibrated MeCN solutions at room temperature. Each dumbbell component in the three [2]rotaxanes contains five distinct chromophoric units—namely, a TTF unit, a DNP moiety, a terphenylene spacer, and two stoppers, the same in 1^{4+} and different in 3^{4+} and 5^{4+} . In addition, all three of the [2]rotaxanes contain, of course, the CBPQT^{4+} ring which consists of two equivalent and non-interacting^[33] bipyridinium chromophoric units.

Table 1. MS data for the [2]rotaxanes $1\cdot 4\text{PF}_6$, $3\cdot 4\text{PF}_6$ and $5\cdot 4\text{PF}_6$.

[2]Rotaxane	$M^{[a]}$	$[M-\text{PF}_6]^+$	$[M-2\text{PF}_6]^+$	$[M-3\text{PF}_6]^+$	$[M-2\text{PF}_6]^{2+}$	$[M-3\text{PF}_6]^{2+}$	$[M-4\text{PF}_6]^{2+}$	$[M-3\text{PF}_6]^{3+}$	$[M-4\text{PF}_6]^{4+}$
$1\cdot 4\text{PF}_6$ ^[b]	(3020)	–	–	–	1366	1293	–	862	610
$3\cdot 4\text{PF}_6$ ^[c]	(3324)	3179	3034	2888	1517	1445	1372	–	–
$5\cdot 4\text{PF}_6$ ^[c]	(3324)	3178	3035	2889	1517	1446	1372	–	–

[a] The peaks corresponding to the molecular ion were not observed. The molecular weights are shown in parentheses. [b] ESI-MS data. [c] FAB-MS data.

Table 2. Selected chemical shifts (δ values) from the ^1H NMR spectra^[a] of the [2]rotaxanes **1-4**PF₆, **3-4**PF₆ and **5-4**PF₆

[2]Rotaxane	H _{α} ^[b]	TTF Protons ^[b]	-(CH ₂ O) ₃ C ₆ H ₂ CH ₂ O- ^[b]	-CH ₂ -N ⁺ ^[b]
1-4 PF ₆ ^[c]	8.97, 8.87, 8.79	6.23, 6.17, 6.06, 5.98	–	5.76–5.47
3-4 PF ₆ ^[c]	8.95, 8.86, 8.77	6.22, 6.16, 6.06, 5.96	4.90, 4.80	5.71–5.43
5-4 PF ₆ ^[c]	8.88, 8.76, 8.62	6.20, 6.10, 5.98, 5.92	4.80, 4.74	5.66–5.32

[a] The ^1H NMR spectra were recorded at 500 MHz in CD₃CN at ambient temperature with concentrations of approximately 1 mM. [b] The protons mentioned are depicted on the structural formulas in Figure 1. [c] The ^1H NMR spectra corresponding to **1-4**PF₆, **3-4**PF₆, and **5-4**PF₆ are shown in a), b), and c), respectively, in Figure 9.

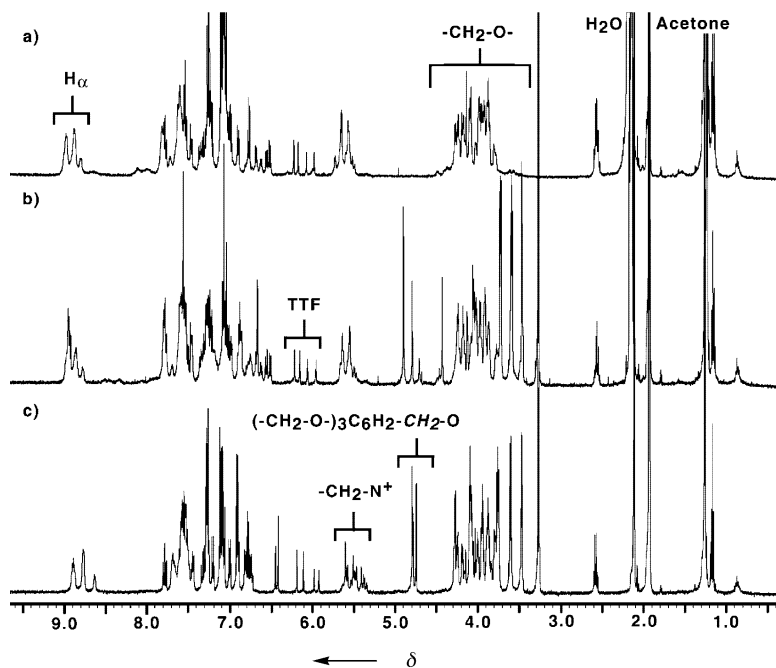


Figure 3. ^1H NMR Spectra of the rotaxanes a) **1-4**PF₆, b) **3-4**PF₆ and c) **5-4**PF₆ recorded in CD₃CN at 500 MHz at room temperature.

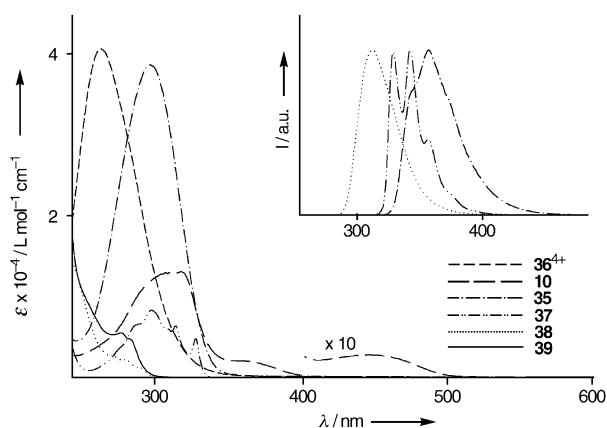


Figure 4. Absorption spectra of the free cyclophane **36**⁴⁺ and of the model compounds of the chromophoric units incorporated in dumbbell-shaped compounds **2**, **4**, and **6**. The emission spectra of the fluorescent compounds **35**, **37**, and **38** are shown in the inset (air equilibrated MeCN solution, room temperature).

The photophysical investigations were carried out on three major groups of compounds, i) the reference compounds, namely the cyclophane^[17] CBPQT⁴⁺ (**36**⁴⁺) and the

model compounds **10**, **35**, **37**,^[25] **38**,^[19] and **39**^[26] (Figure 2), ii) the dumbbell compounds **2**, **4**, and **6**, and iii) the model [2]rotaxane **1**⁴⁺ and the constitutionally isomeric [2]rotaxanes **3**⁴⁺ and **5**⁴⁺.

*Cyclophane CBPQT*⁴⁺ (**36**⁴⁺) and model compounds **10**, **35**, **37**, **38**, and **39**: The absorption spectra of **36**⁴⁺ and the model compounds, serving as references for the appropriate chromophore units of the dumbbell components **2**, **4**, and **6** are shown in Figure 4. None of these compounds shows absorption bands in the visible region with the exception of compound **10** which has a very weak absorption band with a maximum at around 450 nm. Compounds **35**, **37**, and **38** display, as expected,^[34] strong fluorescence bands in the region of 300–400 nm (Figure 4, inset) whereas compound **10**, the cyclophane **36**⁴⁺ and compound **39** do not show any emission. The lack of emission by **39**, which contains potentially fluorescent aryloxy subunits, has been noted previously.^[19] The lowest energy emission band ($\lambda_{\text{max}} = 360$ nm) is that exhibited

by the dialkoxyterphenylene spacer **35**: it is characterized by a very high quantum yield (0.95) and a short lifetime (1.4 ns).

Dumbbells 2, 4, and 6: The absorption spectra of the dumbbell compounds **2**, **4**, and **6** are very similar to the sum of the spectra of the model compounds **10**, **35**, **37**, **38**, and **39** for their component units. None of the dumbbells, however, exhibit any emission, which shows that the potentially fluorescent excited states of components **35**, **37**, and **38** are quenched very efficiently.^[35] This observation indicates that, in the ground state, there is no significant intramolecular interaction among the various chromophoric groups present in the dumbbell compounds. This result is not unexpected since, in the dumbbells, the lowest excited state is that of the non-emitting TTF unit^[22b] as shown by the absorption spectra displayed in Figure 4. In fact, i) the fluorescent excited states of the DNP moiety and the aryloxy units of the tetraarylmethane stopper reference compounds **37** and **38**, respectively, can be quenched efficiently by Förster-type energy transfer^[36] since their emission bands overlap the absorption bands of the TTF and spacer model compounds **10** and **35**, respectively, and ii) the fluorescent excited state of the terphenylene reference compound **35**, in its turn, can be

quenched efficiently since its fluorescence band overlaps the absorption band of the TTF compound **10**. Moreover, a reductive electron transfer of the excited states of the DNP moiety, the terphenylene spacer, and the hydrophobic stopper by the ground state of the TTF unit can also be expected in view of its low oxidation potential (+0.35 V vs SCE) and the high energies of the excited states.

[2]Rotaxanes 1⁴⁺, 3⁴⁺, and 5⁴⁺: A comparison between the absorption spectra of the rotaxanes **1⁴⁺**, **3⁴⁺**, and **5⁴⁺** with the sum of the spectra of the CBPQT⁴⁺ cyclophane and of the respective dumbbells, **2**, **4**, and **6** shows that there are small differences in the UV spectral region and a generally higher absorbance in the rotaxane spectra above 350 nm, characterized by a broad and relatively weak band with $\lambda_{\text{max}}=840$ nm (see, for example, Figure 5). Such an absorp-

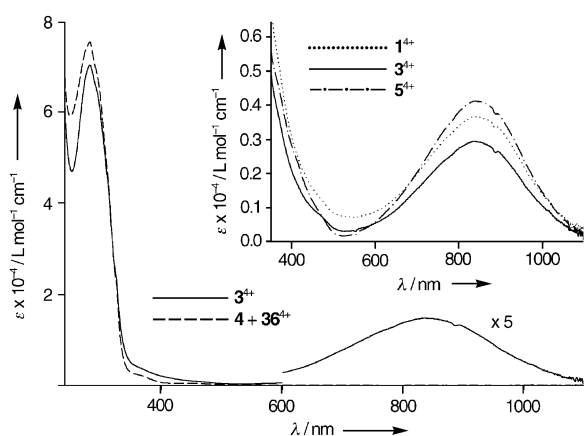


Figure 5. Comparison of the absorption spectrum of [2]rotaxane **3⁴⁺** (solid line) and the sum (dashed line) of the spectra of its dumbbell (**4**) and ring (**36⁴⁺**) components. The inset shows the CT region of the absorption spectra of the [2]rotaxanes **1⁴⁺**, **3⁴⁺** and **5⁴⁺** (MeCN solution, room temperature).

tion band is typical of charge transfer (CT) interactions arising when a TTF unit is encircled by the CBPQT⁴⁺ cyclophane.^[22b] It is also known that the CT interaction, arising when the CBPQT⁴⁺ cyclophane encircles a DNP moiety (which is more difficult to oxidize than a TTF unit), results^[22a] in an absorption band at 520 nm. CT Bands at higher energies are expected to arise from the interactions between the cyclophane CBPQT⁴⁺ and other, weaker electron-donor units present within the dumbbells. It should be noted (inset in Figure 5) that the spectra of the three rotaxanes **1⁴⁺**, **3⁴⁺**, and **5⁴⁺** in the CT region are similar but not identical. The presence of absorption bands with maxima at 840 nm and the absence of bands around 520 nm demonstrate that, in all cases, by far the most predominant, if indeed not the only, translational isomer populated is the one in which the CBPQT⁴⁺ cyclophane encircles the TTF unit as portrayed by the structural formulas shown in Figure 1. This conclusion is entirely consistent with the results obtained from ¹H NMR spectroscopy (see above) and electrochemistry

(see below). The non-negligible absorbance in the 350–550 nm region shows, however, that the CBPQT⁴⁺ cyclophane, while encircling the TTF unit, is also involved in CT interactions with other electron-donor residues. This observation is consistent with folded conformations; their presence is also indicated by the results of ¹H NMR spectroscopic and electrochemical experiments. In view of the small differences in the absorbance values and the wide variety of possible CT interactions that can arise in folded conformations, we believe that further speculation concerning which moiety (or moieties) of the dumbbells is (are) engaged in alongside interactions with the CBPQT⁴⁺ cyclophane would be premature. The existence of folded conformations could also affect the interaction between the CBPQT⁴⁺ cyclophane and the encircled TTF units, a situation which could account for the differences in the values of the molar absorption coefficients for the three rotaxanes at 840 nm.

Electrochemical investigations: Electrochemical experiments—namely, cyclic voltammetry (CV) and differential pulse voltammetry (DPV)—were carried out in argon-purged MeCN solutions at room temperature. All potential values are referred to SCE. Since the redox-active bistable rotaxanes **1⁴⁺**, **3⁴⁺**, and **5⁴⁺** contain several electrochemically active units, they display a rather complex electrochemical behavior. In order to render a potentially daunting task a practical one, we have focused our investigations on the oxidation processes associated with the π -electron-rich units, that is, the TTF unit and the DNP moiety, in the dumbbell components, and on the reduction processes involving the π -electron deficient bipyridinium units of the cyclophane component. For comparison purposes, the electrochemical properties of the free dumbbell compounds **2**, **4**, and **6**, the free cyclophane **36⁴⁺** and the model compounds **10**, **35**, **37**, **38**, and **39** for the electro-active units contained in the dumbbells have also been investigated. Some of the results from the electrochemical investigations are summarized in Table 3.

Table 3. Electrochemical data^[a] for the TTF and DNP model compounds **10** and **37**, the dumbbell compounds **2**, **4**, and **6**, the ring component CBPQT⁴⁺ and the [2]rotaxanes **1⁴⁺**, **3⁴⁺**, and **5⁴⁺**.

Compounds	TTF ^[b]		DNP ^[b]		4,4'-bipyridinium ^[b]	
	E_{ox} [V]	E_{ox} [V] ^[c]	E_{ox} [V] ^[c]	E_{ox} [V] ^[c]	E_{red} [V]	E_{red} [V]
10	+0.35	+0.71	–	–	–	–
37	–	–	+1.17	–	–	–
dumbbell 2	+0.35	+0.72	+1.17	–	–	–
dumbbell 4	+0.35	+0.73	+1.17	–	–	–
dumbbell 6	+0.35	+0.73	+1.18	–	–	–
CBPQT ⁴⁺	–	–	–	–	–0.29 ^[d]	–0.71 ^[d]
[2]rotaxane 1⁴⁺	+0.74 ^[d,e]	>+1.30	>+1.30	–0.30	–0.37	–0.82 ^[d]
[2]rotaxane 3⁴⁺	+0.74 ^[d,e]	>+1.30	>+1.30	–0.31	–0.36	–0.81 ^[d]
[2]rotaxane 5⁴⁺	+0.73 ^[d,e]	>+1.30	>+1.30	–0.31	–0.40	–0.83 ^[d]

[a] Argon-purged MeCN, room temperature, tetraethylammonium hexafluorophosphate (TEAPF₆) as supporting electrolyte, glassy carbon as working electrode; potential values in V vs. SCE; reversible and mono-electronic process, unless otherwise indicated. [b] Unit involved in the observed process. [c] Irreversible process; potential value estimated by the DPV peak. [d] Bielectronic process. [e] Process affected by kinetic complications; potential value estimated by the DPV peak.

Model compounds 10, 35, 37, 38, and 39: These five compounds undergo only oxidation processes in the potential window examined ($-2.0/+2.0$ V). Compound **10**, a model for a free TTF unit, exhibits (Table 3) two one-electron reversible oxidation processes at $+0.35$, $+0.71$ V, characteristic of TTF.^[38] Compound **37** shows (Table 3) an irreversible oxidation process at $+1.17$ V, that can be easily assigned to the DNP moiety.^[22b,37] The other model compounds for the terphenylene spacer **35**, the tetraarylmethane hydrophobic stopper **38** and the dendritic hydrophilic stoppers **39** can only be oxidized at higher potentials: three oxidation processes at $+1.29$, $+1.43$ and $+1.52$ V, two at $+1.55$ and $+1.76$ V, and four at $+1.27$, $+1.32$, $+1.59$ and $+1.73$ V were obtained, respectively, for compounds **35**, **38**, and **39**.

Dumbbell compounds 2, 4, and 6 and the CBPQT⁴⁺ cyclophane 36⁴⁺: The free dumbbell compounds **2**, **4**, and **6** exhibit several oxidation processes. The two reversible and mono-electronic processes observed at $+0.35$ and $+0.72$ V can be assigned clearly to the TTF unit by comparison with the model compound **10**, and the irreversible process that follows at $+1.17$ V can be assigned to the DNP moiety by comparison with the behavior of the reference compound **37** (Table 3). At more positive potentials, several overlapping processes, related to the oxidation of the spacer and stoppers, can be observed. In conclusion, the electrochemical properties of the dumbbell components are those expected from the redox behavior of their model compounds, without evidence of inter-component interactions. The electron-accepting cyclophane CBPQT⁴⁺ shows (Table 3) the well-known^[21a,22b,33,39] reversible and bielectronic reduction processes at -0.29 and -0.71 V which can be assigned to the first and, respectively, second reduction of the two equivalent non-interacting bipyridinium units.

[2]Rotaxanes 1⁴⁺, 3⁴⁺, and 5⁴⁺: Prior to an analysis of the results obtained for these three redox-active, bistable [2]rotaxanes, it is worth contemplating the anticipated effects upon the redox processes of the cyclophane and dumbbell components brought about by their being interlocked. The oxidation of a TTF unit or a DNP moiety is strongly conditioned by the presence of an encircling CBPQT⁴⁺ because of i) the presence of donor–acceptor interactions and ii) the strong electrostatic repulsion arising between the generated radical cation and the tetracationic cyclophane. The oxidation of the encircled TTF unit or DNP moiety should hardly be affected, however, by conformational folding because of the shielding effect provided by the surrounding tetracationic cyclophane toward external interactions. By contrast, it is known that the reduction of the **36⁴⁺** cyclophane is weakly influenced by threading an uncharged electron donor because electrostatic effects are not involved. However, the reduction processes should be affected by folding since the highly charged cyclophane is strongly exposed to external interactions.^[21,33] It follows that the oxidation processes should give information on the nature of the translational isomerism and, when appropriate, on the occurrence of shuttling movements, whereas the reduction processes should reveal the occurrence of conformational folding.

1) Oxidation processes: For the rotaxanes **1⁴⁺**, **3⁴⁺**, and **5⁴⁺**, the first oxidation process (Table 3 and Figure 6) is bielectronic and occurs at $+0.74$ V. This result shows that the two reversible and mono-electronic oxidation processes associat-

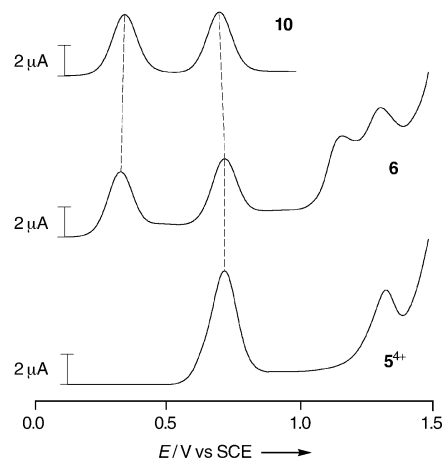


Figure 6. Anodic DPV patterns of the model compound **10**, the dumbbell compound **6** and the [2]rotaxane **5⁴⁺**. The current intensities have been corrected to take into account differences in concentrations and diffusion coefficients (Argon purged MeCN solution, room temperature, scan rate 4 mV s^{-1} , pulse height 10 mV).

ed with the TTF unit, which are well separated in the model compound **10**, as well as in the dumbbells **2**, **4**, and **6**, take place at the same potential. The lack of an oxidation process taking place around $+0.35$ V, at least within the limits of the experimental error, and the large shift (ca. 400 mV) toward more positive potential values of the first oxidation process, shows that, in each rotaxane, there is only one translational isomer that is populated—namely, that in which the CBPQT⁴⁺ cyclophane encircles the TTF unit. The electron-accepting tetracationic cyclophane increases the first oxidation potential of the encircled TTF unit for two reasons—i) it engages the TTF unit in donor–acceptor interactions and ii) it makes more difficult the formation of a monocationic TTF^{•+} species inside the cyclophane. The second oxidation process of the TTF unit in the rotaxanes takes place (Table 3 and Figure 6) at the same potential value as that of the corresponding dumbbell. This result and the observation that the cyclic voltammetric pattern corresponding to the TTF unit is affected by kinetic complications demonstrate that, after the first oxidation process involving the TTF unit, the CBPQT⁴⁺ cyclophane moves away from this unit. It should also be noted (Table 3 and Figure 6) that, in all three rotaxanes, the oxidation of the DNP moiety is shifted toward more positive potential values, compared to those observed in the dumbbells. Although, in all cases, the exact potential associated with the DNP oxidation process is difficult to establish, because of the presence of processes involving other units of the dumbbell above $+1.30$ V, the observed shift shows that, after TTF oxidation, the CBPQT⁴⁺ cyclophane moves onto the DNP moiety, thereby destabilizing the formation of its radical cation.^[40] In conclusion, the results obtained from elec-

trochemical oxidation show that, in all three rotaxanes, the CBPQT⁴⁺ cyclophane is originally located around the TTF unit and shuttles between the TTF and DNP “stations” upon ox-red stimulation. These results are fully confirmed by the chemical oxidation/reduction experiments described in the final subsection of this paper. It is interesting to note that the nature and relative positions of the stoppers do not seem to play any role regarding the location of the tetracationic cyclophane and the occurrence of the shuttling process, whereas, in similar rotaxanes^[19] the nature of the stoppers influences the relative populations of the two translational isomers.

2) *Reduction processes*: The CBPQT⁴⁺ cyclophane in MeCN solutions shows^[21a,22b,33,39] two reversible, bielectronic processes at -0.29 and -0.71 V, assigned to the first and, respectively, second reductions of the two equivalent and non-interacting bipyridinium units. The electrochemical properties of CBPQT⁴⁺ (**36**⁴⁺) are known to change when this cyclophane is threaded by a π -electron donor. The first bielectronic reduction process is expected to and, in fact, does i) move slightly toward more negative potential values in pseudorotaxanes^[41] and rotaxanes,^[35b] and ii) split into two distinct processes in catenanes^[21a,22b,33] in which the two bipyridinium units are topologically non-equivalent. Splitting, however, has also been observed in the case of some pseudorotaxanes^[22b] and rotaxanes.^[19,42]

For the rotaxanes **1**⁴⁺, **3**⁴⁺, and **5**⁴⁺ the first bielectronic reduction process of the tetracationic cyclophane splits (Table 3 and Figure 7) into two distinct processes, indicating that the equivalence of the two bipyridinium units is lost. This result can be accounted for by assuming that the cyclophane, while encircling the TTF unit, is also involved in other non-symmetric alongside interactions. Such behavior requires the presence of folded conformations, an explanation previously advanced for other long and flexible pseudorotaxanes^[22b] and rotaxanes.^[19] Interestingly, whereas the presence of folded conformations is required to explain the splitting of the first bielectronic reduction for each one of the three rotaxanes, a detailed examination of the electrochemical data shows that each compound displays some peculiar features. Since the three rotaxanes differ only in the nature and relative positions of the stoppers, it seems likely that these appendages are directly involved in determining the observed differences.

In the case of the rotaxane **1**⁴⁺, which contains two identical tetraarylmethane stoppers, deconvolution of the DPV peaks shows (Figure 7) that the first reduction process occurs at -0.30 V, that is, at a potential slightly more negative than that (-0.29 V) of the free CBPQT⁴⁺, but slightly less negative than that expected^[22b,41] for a bipyridinium unit engaged in CT interactions with a threaded TTF unit. The second process occurs at a considerably more negative potential (-0.37 V), suggesting that there are bipyridinium units that are also involved in alongside interactions in folded conformations. Deconvolution of the DPV shows also that the first and second processes account for 1.3 and 0.7 exchanged electrons, respectively, indicating that 35% of the bipyridinium units are involved in the folded in-

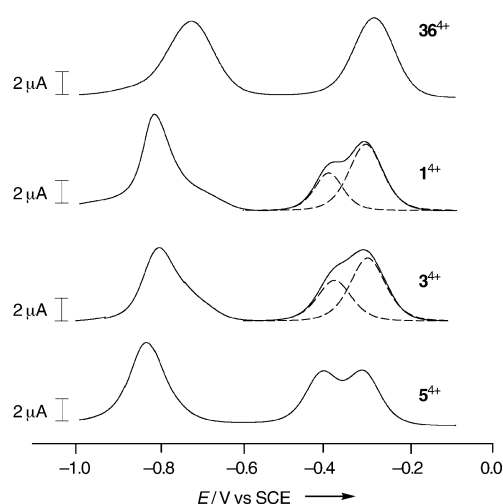


Figure 7. Cathodic DPV patterns of the cyclophane **36**⁴⁺ and of the [2]rotaxanes **1**⁴⁺, **3**⁴⁺ and **5**⁴⁺. The current intensity has been corrected to take into account differences in concentrations and diffusion coefficients (Argon purged MeCN solution, room temperature, scan rate 4 mVs^{-1} , pulse height 10 mV).

teractions. Interestingly, the successive reduction of the two bipyridinium units of the cyclophane takes place at the same potential which is shifted toward more negative values compared with (Table 3) the free tetracationic cyclophane.^[43] This result shows that, after the first reduction process, the two bipyridinium units still interact with π -electron-donating units, but then become equivalent, suggesting that unfolding takes place after one-electron reduction of the two bipyridinium units.

That electrochemical stimulation can cause not only shuttling, but also conformational folding and unfolding processes in long and flexible rotaxanes is a novel, yet clearly not unexpected result, since such folding and unfolding processes in proteins are known^[44] to be redox controlled.

The behavior (Table 3 and Figure 7) of the rotaxane **3**⁴⁺ is very similar, but not identical to that of **1**⁴⁺. Replacement of the tetraarylmethane stopper, which is distant from the tetracationic cyclophane encircling the TTF unit with an aryloxy dendritic stopper apparently has a very weak perturbing effect.

In the case of the rotaxane **5**⁴⁺, the first process takes place (Table 3 and Figure 7) at a potential similar to that of **1**⁴⁺ and **3**⁴⁺, while the second process is displaced toward more negative potentials. Furthermore, the first and second processes observed in the case of **5**⁴⁺ involve an electron each, suggesting that, in this rotaxane, 50% of the bipyridinium units are engaged in folding interactions. The different behavior of the constitutionally isomeric rotaxanes **3**⁴⁺ and **5**⁴⁺ confirms the presence of folded conformations and demonstrates that the dendritic stopper plays a more important role when it is closer to the tetracationic cyclophane. The successive reduction of the two bipyridinium units occurs at the same potential also in rotaxane **5**⁴⁺ indicating that, once again, after the first reduction, unfolding occurs.

Chemical oxidation/reduction and shuttle control: It is known^[22] that TTF can be oxidized stoichiometrically to the mono and dicationic forms, $\text{TTF}^{+\cdot}$ and TTF^{2+} , by Fe^{III} perchlorate. Such an oxidation process can be followed by changes in the absorption spectra^[45] ($\text{TTF}^{+\cdot}$: $\lambda = 434 \text{ nm}$, $\epsilon = 15000 \text{ M}^{-1} \text{ cm}^{-1}$ and $\lambda = 577 \text{ nm}$, $\epsilon = 4000 \text{ M}^{-1} \text{ cm}^{-1}$; TTF^{2+} : $\lambda = 348 \text{ nm}$, $\epsilon = 9000 \text{ M}^{-1} \text{ cm}^{-1}$). We have verified that the TTF units contained within compound **10** and the dumbbell components **2**, **4**, and **6**, as well as the rotaxanes **1**⁴⁺, **3**⁴⁺, and **5**⁴⁺, can be oxidized stoichiometrically by Fe^{III} perchlorate. In the rotaxanes, the absorption band with $\lambda_{\text{max}} = 840 \text{ nm}$, assigned to the CT interactions between the TTF unit and the tetracationic cyclophane, disappears (Figure 8) upon addition of a stoichiometric amount of Fe^{III} perchlo-

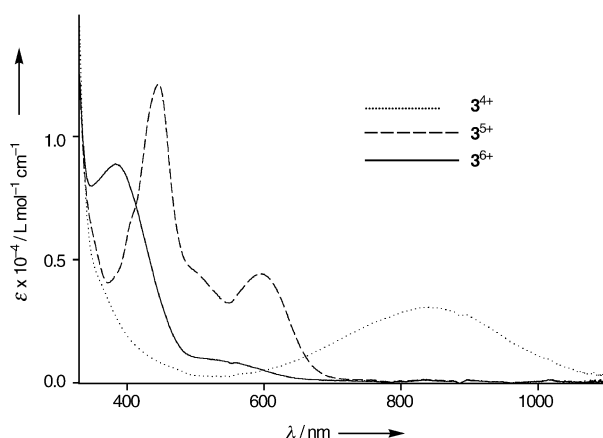


Figure 8. Absorption spectra of the [2]rotaxane **3**⁴⁺ and of its mono- and di-oxidized forms **3**⁵⁺ and **3**⁶⁺ obtained by $\text{Fe}(\text{ClO}_4)_3$ oxidation of the TTF station in MeCN. Addition of silver powder to the oxidized solutions restores the original spectrum.

rate. An isobestic point is maintained at $\lambda = 645 \text{ nm}$ throughout the titration. Addition of a second equivalent of Fe^{II} leads to the two-electron oxidized species with an isobestic point at 415 nm. These processes are reversible. Addition of silver powder regenerates the starting species. When the spectra of mono-oxidized dumbbells are subtracted from the spectra of the corresponding mono-oxidized rotaxanes, weak absorption bands with maxima at about 520 nm are obtained, confirming that the tetracationic cyclophane shuttles between the TTF and DNP “stations” upon ox/red stimulation.

Previously, some of us had described^[23] how the chemically controlled shuttling of the rotaxane **1**⁴⁺ could be monitored by ¹H NMR spectroscopy. In order to confirm the fact that the addition of the hydrophilic stopper has no major effect on the redox-based chemical switching, an identical procedure was performed on the rotaxane **5**⁴⁺. After recording the ¹H NMR spectrum (Figure 9a) in CD_3CN at 243 K, 2.2 equivalents of the oxidant, tris(*p*-bromophenyl)amminium hexafluoroantimonate were added.^[46] The low temperature was employed to ensure the stability of the oxidized rotaxane. When the ¹H NMR spectrum was recorded again

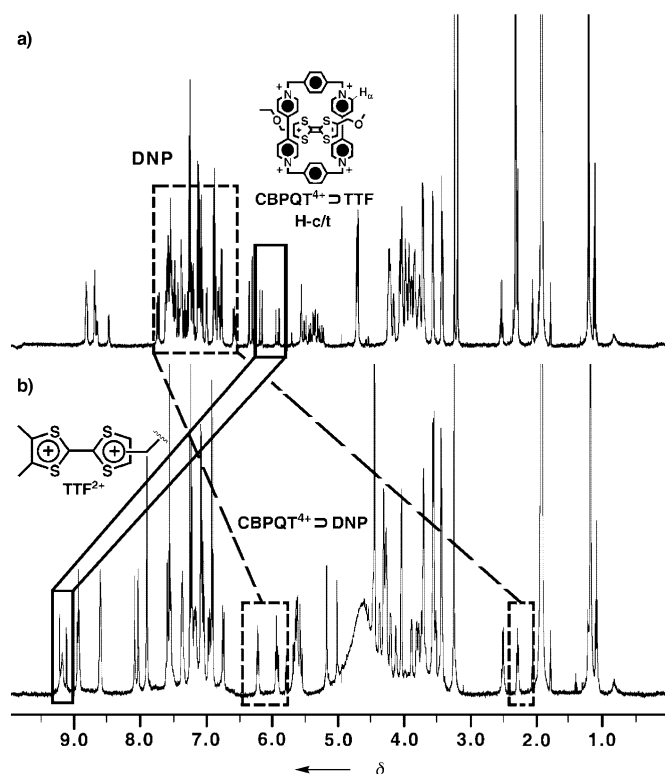


Figure 9. a) ¹H NMR Spectrum recorded at 500 MHz for the [2]rotaxane **5**⁴⁺ in CD_3CN at 243 K. The solid box highlights the peaks for the H-c/t (*cis/trans*) in the neutral TTF unit encircled by the CBPQT^{4+} cyclophane. The dashed box highlights the region that contains the resonances for the ring protons of the DNP system that is “free” in **5**⁴⁺. b) ¹H NMR Spectrum recorded at 500 MHz of the bis-oxidized **5**⁶⁺ in CD_3CN at 243 K. The solid box highlights the peaks for the “free” dicationic TTF^{2+} residues and the dashed boxes indicate the peaks for H-2/6 and H-3/7 (at lower field) and for H-4/8 (at higher field) in the DNP ring system encircled by the CBPQT^{4+} cyclophane.

(Figure 9b) after this oxidation, the signals for the heterotopic protons on the TTF unit were observed to move from δ 6.15, 6.19, 6.30, and 6.35—reflecting the fact that the TTF unit in **5**⁴⁺ is in its slowly interconverting *cis* and *trans* isomeric states and encircled by the CBPQT^{4+} ring—to δ 9.12 and 9.22, characteristic of the free TTF^{2+} dication in the oxidized version of the rotaxane. Further evidence for the translation of the CBPQT^{4+} ring from the oxidized TTF unit to the DNP moiety can be found in the dramatic changes of the chemical shifts of the DNP protons. In the starting rotaxane **5**⁴⁺, the resonances appear at δ 6.86 and 6.88 (H-4/8), δ 7.28 and 7.32 (H-3/7) and δ 7.72 and 7.74 (H-2/6) as expected. Upon oxidation of the rotaxane, the signals for the DNP moiety experience large upfield shifts to δ 2.28 and 2.29 (H-4/8), δ 5.92 and 5.94 (H-3/7), and δ 6.21 and 6.23 (H-2/6) on account of the shielding effect of the encircling CBPQT^{4+} ring. Reduction with zinc dust restores the original spectrum. The chemically controlled shuttling, within the rotaxane **5**⁴⁺, of the CBPQT^{4+} ring between the dumbbell’s TTF and DNP “stations”, on oxidation of the TTF unit and its subsequent reduction, is summarized in Figure 10.

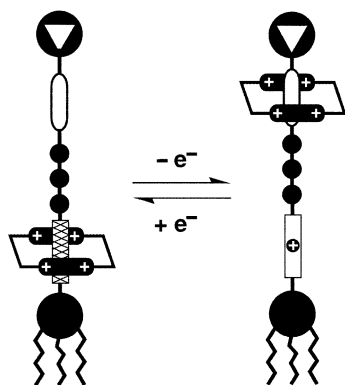


Figure 10. Idealized graphical representation of redox switching in the amphiphilic, bistable [2]rotaxane 5^{4+} .

Conclusion

A systematic photophysical, electrochemical and spectroscopic investigation of the three [2]rotaxanes introduced in Figure 1 has indicated that, although the nature and relative positions of the hydrophobic and hydrophilic stoppers do not appear to have any noticeable effect on the shuttling properties of the rotaxanes, they do play a perceptible role in the formation of folded conformations wherein presumably stopper components interact in a stabilizing manner with the exterior surface of the ring component. Whereas ox/red stimulation of the tetrathiafulvalene “station” causes shuttling of the tetracationic cyclophane between the dumbbell’s two “stations”, ox/red stimulation of the cyclophane initiates the unfolding/folding processes. These results are important in the context of designing, synthesizing and fabricating nanoscale systems and devices. Since the mechanically active molecules come into contact with substrates and electrodes in nanoscale systems and solid-state devices, it is unlikely that all their fine solution-state, structural features will be carried over into the condensed matter phase^[47] (Figure 11). Nonetheless, forewarned of complexity means prepared for the unexpected.

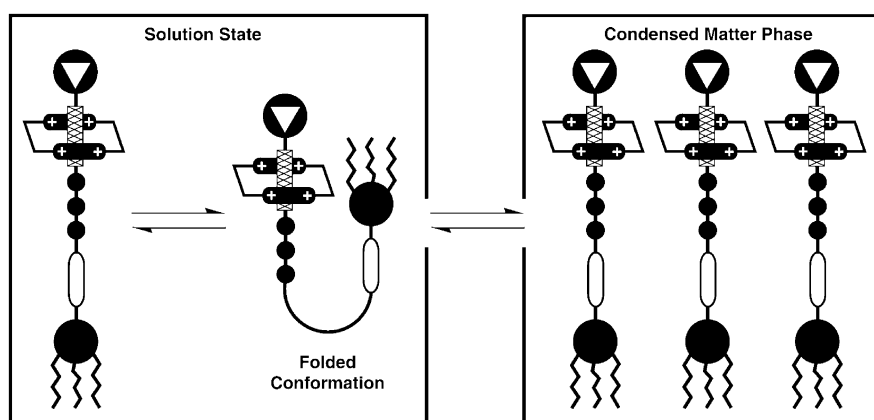


Figure 11. Idealized graphical representations drawing attention to the possible differences between amphiphilic, bistable [2]rotaxane molecules a) equilibrating between folded and unfolded conformations in the solution state, and b) self-organized in a condensed matter phase.

Experimental Section

General methods: Chemicals were purchased from Aldrich and used as received. The compounds 4,4'(5')-bis(hydroxymethyl)- $\Delta^{2,2}$ -bi-1,3-dithiole^[28] (**7**), 2-[2-(2-iodoethoxy)-ethoxy]tetrahydropyran^[29] (**8**), 4-[bis(4-*tert*-butylphenyl)-(4-ethylphenyl)methyl]phenol^[27] (**12**), compound^[16] **15**, α,α' -[1,4-phenylenebis(methylene)]bis(4,4'-bipyridium) bis(hexa-fluorophosphate)^[30] (**22-2 PF₆**), 2-(2-[5-[2-(2-hydroxy-ethoxy)ethoxy]naphthalen-1-yloxy]ethoxy)ethanol^[25] (**24**), the dendritic hydrophilic stopper^[11c,26] **31** and [1,1':4',1'']terphenyl-4,4''-diol^[31] (**33**) were all prepared according to literature procedures. Solvents were dried following methods described in the literature.^[48] All reactions were carried out under an anhydrous argon atmosphere. Thin-layer chromatography (TLC) was performed on aluminum sheets coated with silica gel 60F (Merck 5554). The plates were inspected by UV light and, if required, developed in I_2 vapor. Column chromatography was carried out by using silica gel 60 (Merck 9385, 230–400 mesh). Melting points were determined on an Electrothermal 9100 melting point apparatus and are uncorrected. All 1H and ^{13}C NMR spectra were recorded on either i) a Bruker ARX400 (400 MHz and 100 MHz, respectively), ii) a Bruker ARX500 (500 MHz and 125 MHz, respectively) or iii) a Bruker Avance500 (500 MHz and 125 MHz, respectively), using residual solvent as the internal standard. Samples were prepared using $CDCl_3$, CD_3COCD_3 or CD_3CN purchased from Cambridge Isotope Labs. All chemical shifts are quoted using the δ scale, and all coupling constants (J) are expressed in Hertz (Hz). Fast atom bombardment (FAB) mass spectra were obtained using a ZAB-SE mass spectrometer, equipped with a krypton primary atom beam utilizing a *m*-nitrobenzyl alcohol matrix. Cesium iodide or poly(ethylene glycol) were employed as reference compounds. Electro spray mass spectra (ESMS) were measured on a VG ProSpec triple focusing mass spectrometer with MeCN as the mobile phase. Microanalyses were performed by Quantitative Technologies, Inc.

Compound 10: A solution of the iodide **8** (9.09 g, 30.3 mmol) in THF (200 mL) was added dropwise under an Ar atmosphere to a solution (900 mL) of the diol **7** (2.00 g, 7.89 mmol) and NaH (1.39 g, 60.6 mmol) in THF (900 mL) and the reaction mixture was heated under reflux for 1 h. The mixture was then stirred under reflux for 48 h before being cooled down to room temperature. After the addition of MeOH (20 mL), the mixture was filtered through silica gel and the solution was evaporated in vacuo to obtain the crude compound **9** as a brown oil which was dissolved in MeOH/ CH_2Cl_2 (1:1, 200 mL). A conc. HCl aqueous solution (0.5 mL) was added and the reaction mixture was stirred at room temperature for 2 h. 1 N NaOH aqueous solution (200 mL) was added to the reaction mixture and it was extracted by CH_2Cl_2 (3×100 mL) and dried ($MgSO_4$). After removal of the solvent, the residue was purified by column chromatography (silica gel: $CH_2Cl_2/MeOH$ 100:3) to give the diol **10** (2.08 g, 60%) as an orange oil. 1H NMR (CD_3CN , 400 MHz): δ = 2.48 (br, 2H), 3.30–3.60 (m, 16H), 4.26 (s, 4H), 6.38 (s, 2H); ^{13}C NMR (CD_3CN , 100 MHz): δ = 62.0, 68.6, 70.2, 70.9, 73.4, 117.8, 117.9, 118.3, 135.5, 135.6; MS (FAB): m/z (%): 440 (100) [M]⁺.

Monotosylate 11: A solution of TsCl (634 mg, 3.3 mmol) in CH_2Cl_2 (10 mL) was added dropwise to a solution of the diol **10** (1.63 g, 3.7 mmol), Et_3N (2.57 mL, 18.5 mmol) and DMAP (15 mg) in CH_2Cl_2 (90 mL) at 0°C. The mixture was then stirred for 16 h at room temperature. After addition of Al_2O_3 (10 g, neutral, Brockmann I), the mixture was evaporated and subjected to column chromatography (silica gel: $CH_2Cl_2/EtOH$ 100:3). The second yellow band was collected to give the monotosylate **11** (989 mg, 45%) as a yellow oil. 1H NMR (CD_3CN , 500 MHz): δ = 2.42 (s, 2H), 2.74 (t, 1H, J = 3.7 Hz), 3.45–3.47 (m, 6H), 3.53–3.60 (m, 8H), 4.09 (t, 2H, J = 4.3 Hz), 4.21 (s, 2H), 4.25 (s, 2H), 6.34 (s, 1H), 6.37 (s, 1H), 7.41 (d, 2H, J =

8 Hz), 7.76 (d, 2H, $J=8$ Hz); ^{13}C NMR (CD_3CN , 125 MHz): $\delta=20.6$, 60.7, 68.1, 68.9, 69.1, 69.8, 69.9, 72.2, 116.7, 116.8, 127.7, 129.9, 132.7, 134.4, 134.5, 134.6, 145.3; MS (FAB): m/z (%): 748 (6) $[M]^+$, 594 (51), 307 (100).

Compound 13: A solution of the monotosylate **11** (990 mg, 1.67 mmol), the tetraarylmethane stopper **12** (2.38 g, 5.00 mmol), K_2CO_3 (1.38 g, 10 mmol), LiBr (10 mg), and [18]crown-6 (10 mg) in dry MeCN (50 mL) was heated under reflux for 16 h. After cooling down to room temperature, the reaction mixture was filtered and the residue was washed with MeCN (50 mL). The combined organic phase was concentrated in vacuo and the crude product was purified by column chromatography (silica gel: $\text{CH}_2\text{Cl}_2/\text{EtOH}$ 100:3) to give compound **13** (1.59 g, 95%) as a yellow solid. M.p. 40–42 °C; ^1H NMR (CDCl_3 , 500 MHz): $\delta=1.16$ (t, $J=7.5$ Hz, 3H), 1.25 (s, 18H), 2.57 (q, $J=7.5$ Hz, 2H), 2.70 (brs, 1H), 3.40–3.47 (m, 2H), 3.52–3.61 (m, 10H), 3.71–3.74 (m, 2H), 4.03–4.05 (m, 2H), 4.20–4.25 (m, 4H), 6.30, 6.33 (2×s, 2H), 6.75–6.78 (m, 2H), 7.06–7.13 (m, 10H), 7.23–7.27 (m, 4H); ^{13}C NMR (CD_3CN , 125 MHz): $\delta=14.8$, 25.1, 27.6, 30.4, 33.8, 60.9, 63.0, 67.3, 67.4, 69.1, 69.2, 69.8, 70.0, 70.1, 70.2, 72.2, 113.3, 116.6, 116.7, 116.7, 124.3, 126.9, 130.2, 130.5, 131.6, 134.5, 134.6, 139.5, 141.5, 144.4, 144.7, 148.3, 156.6; MS (FAB): m/z (%): 898 (42), $[M]^+$, 383 (100); elemental analysis calcd (%) for $\text{C}_{51}\text{H}_{62}\text{O}_6\text{S}_4$ (898): C, 68.11; H, 6.95; found: C 67.99, H 5.65.

Compound 14: A solution of compound **13** (853 mg, 0.95 mmol), TsCl (362 mg, 1.9 mmol), DMAP (10 mg) and Et_3N (1.1 mL, 7.6 mmol) in anhydrous CH_2Cl_2 (50 mL) was stirred for 16 h at room temperature. After addition of Al_2O_3 (5 g, neutral, Brockmann I), the mixture was concentrated and the residue was subjected to column chromatography (silica gel: $\text{CH}_2\text{Cl}_2/\text{EtOH}$ 100:3). The first yellow band was collected and afforded compound **14** (880 mg, 88%) as a yellow solid. M.p. 45–47 °C; ^1H NMR (CD_3CN , 500 MHz): $\delta=1.17$ (t, $J=7.6$ Hz, 3H), 1.27 (s, 18H), 2.40 (s, 3H), 2.57 (q, $J=7.6$ Hz, 2H), 3.45–3.48 (m, 4H), 3.55–3.62 (m, 6H), 3.73 (t, $J=4.7$ Hz, 2H), 4.03–4.05 (m, 2H), 4.09–4.12 (m, 2H), 4.17–4.19 (m, 2H), 4.22 (m, 2H), 6.26, 6.29 (2×s, 2H), 6.75–6.78 (m, 2H), 7.05–7.13 (m, 10H), 7.26 (m, 4H), 7.38 (d, $J=8.3$ Hz, 2H), 7.76 (d, $J=8.3$ Hz, 2H); ^{13}C NMR (CDCl_3 , 125 MHz): $\delta=14.6$, 20.6, 27.6, 30.5, 33.8, 63.1, 67.4, 67.5, 68.2, 69.1, 69.3, 69.3, 69.3, 69.7, 70.0, 70.2, 110.0, 110.0, 110.1, 113.4, 113.4, 116.3, 116.4, 116.5, 124.2, 126.7, 127.6, 129.9, 130.2, 130.5, 131.7, 133.1, 134.5, 134.6, 134.6, 134.7, 139.6, 141.6, 144.4, 144.7, 145.1, 148.4, 156.7; MS (FAB): m/z (%): 1052 (50) $[M]^+$, 383 (100); HRMS (MALDI-TOF): calcd for $\text{C}_{58}\text{H}_{68}\text{O}_8\text{S}_5\text{Na}$: 1075.3415; found: 1075.3414.

Compound 17: A mixture of compound **15** (1.72 g, 2.0 mmol), K_2CO_3 (0.42 g, 3.0 mmol) and 4-bromo-(1,1'-biphenyl)-4-ol (**16**) (0.74 g, 3.0 mmol) was suspended in MeCN (20 mL) and heated under reflux for 16 h. After the reaction mixture had been allowed to cool down to room temperature, it was filtered and the residue was washed with MeCN (50 mL). The combined organic phases were concentrated in vacuo and the crude product was purified by column chromatography (silica gel: $\text{CH}_2\text{Cl}_2/\text{MeOH}$ 99:1) to afford compound **17** (1.58 g, 77%) as a white solid. M.p. 133–135 °C; ^1H NMR (CDCl_3 , 500 MHz): $\delta=1.23$ (t, $J=7.6$ Hz, 3H), 1.30 (s, 18H), 2.62 (q, $J=7.6$ Hz, 2H), 3.99 (t, $J=4.8$ Hz, 2H), 4.03 (t, $J=4.8$ Hz, 2H), 4.05–4.10 (m, 4H), 4.15 (t, $J=4.8$ Hz, 2H), 4.21 (t, $J=4.8$ Hz, 2H), 4.30–4.34 (m, 4H), 6.80 (d, $J=8.0$ Hz, 2H), 6.83 (d, $J=8.7$ Hz, 2H), 6.99 (d, $J=8.8$ Hz, 2H), 7.04–7.11 (m, 10H), 7.22 (d, $J=8.6$ Hz, 4H), 7.31 (t, $J=8.7$ Hz, 2H), 7.39 (d, $J=8.6$ Hz, 2H), 7.45 (d, $J=8.6$ Hz, 2H), 7.52 (d, $J=8.6$ Hz, 2H), 7.87 (d, $J=8.7$ Hz, 2H); ^{13}C NMR (CDCl_3 , 125 MHz): $\delta=15.3$, 28.2, 31.4, 34.3, 53.4, 63.1, 67.4, 67.7, 68.0, 68.0, 70.0, 70.0, 70.1, 105.7, 113.2, 114.6, 114.7, 115.1, 120.8, 124.1, 125.1, 126.6, 126.8, 126.8, 127.9, 128.3, 130.7, 131.0, 131.8, 132.2; 139.7, 141.4, 144.2, 144.6, 148.3, 154.3, 154.3, 156.5, 158.6; MS(FAB): m/z (%): 1026 (37) $[M+2]^+$, 1025 (100) $[M+H]^+$, 1024 (39) $[M]^+$.

Preparation of 1.0M Grignard reagent 19: A solution of the 2-(4-bromophenoxy)-tetrahydropyran (**18**) (2.57 g, 10 mmol) and Mg powder (36.5 mg, 15 mmol) in THF (10 mL) was stirred at room temperature for 2 h. A clear 1.0M Grignard reagent **19** in THF was obtained after precipitation of the insoluble inorganic residue.

Compound 21: A solution of the 1.0M Grignard reagent **19** (3 mL, 3 mmol) was added to a solution of **16** (800 mg, 0.8 mmol) and $[\text{Pd}(\text{PPh}_3)_4]$ (80 mg, catalytic amount) in anhydrous THF (10 mL), and the reaction mixture was heated under reflux for 16 h. After cooling

down to room temperature, the solvent was evaporated, yielding compound **20** as a yellow oil, which was then dissolved in CH_2Cl_2 (25 mL). A concentrated aqueous HCl solution (0.5 mL) was added to the mixture and it was stirred at room temperature for another 16 h. H_2O (20 mL) was added and the mixture was extracted with CH_2Cl_2 (3×30 mL) and dried (MgSO_4). After removal of the solvent, the residue was subjected to column chromatography (silica gel: EtOAc/hexanes 1:2) to yield **21** (1.58 g, 71%) as a white solid. M.p. 121–123 °C; ^1H NMR (CDCl_3 , 500 MHz): $\delta=1.31$ (t, $J=7.6$ Hz, 3H), 1.36 (s, 18H), 2.68 (q, $J=7.6$ Hz, 2H), 4.05 (t, $J=4.8$ Hz, 2H), 4.08–4.13 (m, 4H), 4.15 (t, $J=4.8$ Hz, 2H), 4.19–4.22 (m, 2H), 4.27 (t, $J=4.6$ Hz, 2H), 4.36 (t, $J=4.8$ Hz, 2H), 4.39 (t, $J=4.8$ Hz, 2H), 6.86 (d, $J=8.9$ Hz, 2H), 6.89 (d, $J=8.0$ Hz, 1H), 6.90 (d, $J=8.0$ Hz, 1H), 6.94 (d, $J=8.6$ Hz, 2H), 7.05 (d, $J=8.6$ Hz, 2H), 7.10–7.18 (m, 10H), 7.29 (d, $J=8.6$ Hz, 4H), 7.38 (t, $J=8.0$ Hz, 1H), 7.39 (t, $J=8.0$ Hz, 1H), 7.52 (d, $J=8.6$ Hz, 2H), 7.59 (d, $J=8.6$ Hz, 2H), 7.59–7.64 (m, 4H), 7.94 (d, $J=8.0$ Hz, 1H), 7.95 (d, $J=8.0$ Hz, 1H); ^{13}C NMR (CDCl_3 , 125 MHz): $\delta=15.3$, 28.2, 30.9, 31.3, 34.2, 63.1, 67.3, 67.6, 67.9, 67.9, 69.9, 70.0, 70.0, 105.7, 113.1, 114.6, 114.7, 115.0, 115.7, 124.0, 125.1, 126.6, 126.7, 126.9, 126.9, 127.9, 128.1, 130.6, 131.0, 132.2, 133.1, 133.4, 138.9, 139.0, 139.8, 141.3, 144.1, 144.6, 148.2, 154.2, 154.3, 155.3, 156.5, 158.2; MS(FAB): m/z (%): 1038 (20) $[M]^+$, 1025 (15); elemental analysis calcd (%) for $\text{C}_{71}\text{H}_{74}\text{O}_7$ (1038): C 82.05, H 7.18; found: C 82.09, H 7.16.

Compound 2: A solution of compound **21** (727 mg, 0.70 mmol), **14** (733 mg, 0.70 mmol), K_2CO_3 (484 mg, 3.5 mol), LiBr (5 mg) and [18]crown-6 (5 mg) in anhydrous MeCN (20 mL) was heated under reflux for 16 h. After cooling down to room temperature, the reaction mixture was filtered and the residue was washed with MeCN (30 mL). The combined organic phase was concentrated in vacuo and the crude product was purified by column chromatography (silica gel: EtOAc/hexanes 1:2) to give the dumbbell-shaped compound **2** (664 mg, 47%) as a light yellow solid. M.p. 106–108 °C; ^1H NMR (CD_3COCD_3 , 500 MHz): $\delta=1.22$ (t, $J=7.6$ Hz, 6H), 1.31 (s, 36H), 2.63 (q, $J=7.6$ Hz, 4H), 3.62–3.64 (m, 2H), 3.64–3.68 (m, 4H), 3.70–3.73 (m, 2H), 3.79–3.82 (m, 2H), 3.85–3.87 (m, 2H), 3.96 (t, $J=4.8$ Hz, 2H), 4.01 (t, $J=4.8$ Hz, 2H), 4.04 (t, $J=4.7$ Hz, 2H), 4.07 (t, $J=4.7$ Hz, 2H), 4.10–4.13 (m, 2H), 4.18 (t, $J=4.8$ Hz, 2H), 4.20–4.23 (m, 2H), 4.25 (t, $J=4.7$ Hz, 2H), 4.30–4.38 (m, 8H), 6.44, 6.46, 6.47 (3×s, 2H), 6.81–6.86 (m, 4H), 6.94–6.99 (m, 2H), 7.02–7.07 (m, 4H), 7.09–7.20 (m, 18H), 7.30–7.35 (m, 10H), 7.56–7.68 (m, 8H), 7.87 (d, $J=8.3$ Hz, 2H), 7.89 (d, $J=8.3$ Hz, 2H); MS (FAB): m/z (%): 1920 (100) $[M]^+$; elemental analysis calcd (%) for $\text{C}_{122}\text{H}_{134}\text{O}_{12}\text{S}_4$ (1920): C 76.29, H 7.03; found: C 76.13, H 7.06.

[2]Rotaxane 1-4PF₆: A solution of compound **2** (588 mg, 0.31 mmol), the dicationic salt^[30] **22-2PF₆** (648 mg, 0.92 mmol) and α,α' -dibromo-*p*-xylene (**23**) (242 mg, 0.92 mmol) in anhydrous DMF (30 mL) was stirred for 10 d at room temperature. The reaction mixture was subjected directly to column chromatography (silica gel) and unreacted **2** was eluted with Me_2CO , whereupon the eluent was changed to $\text{Me}_2\text{CO}/\text{NH}_4\text{PF}_6$ (1.0 g NH_4PF_6 in 100 mL Me_2CO) and the green band containing **1-4PF₆** was collected. Most of the solvent was removed under vacuum. After adding H_2O (50 mL) to the residue, the precipitate was collected by filtration, washed with Et_2O (30 mL), and dried in vacuo to afford **1-4PF₆** (357 mg, 39%) as a green powder. M.p. 228 °C (decomposed without melting); ^1H NMR (CD_3CN , 500 MHz): $\delta=1.20$ (two triplets, 6H, $J=7.5$ Hz), 1.26–1.30 (m, 36H), 2.61 (q, $J=7.5$ Hz, 4H), 3.82–4.42 (m, 36H), 5.53–5.70 (m, 8H), 6.03, 6.11, 6.22, 6.28 (4×s, 2H), 6.55 (d, $J=8.6$ Hz, 1H), 6.59 (d, $J=8.6$ Hz, 1H), 6.65 (d, $J=8.6$ Hz, 1H), 6.72 (d, $J=8.6$ Hz, 1H), 6.79 (d, $J=8.7$ Hz, 2H), 6.94 (d, $J=8.7$ Hz, 2H), 7.02–7.19 (m, 24H), 7.18–7.45 (m, 10H), 7.50–7.70 (m, 16H), 7.72–7.92 (m, 8H), 8.84–9.01 (m, 8H); MS (ESI): m/z (%): 1366 (23) $[M-2\text{PF}_6]^{2+}$, 862 (40) $[M-3\text{PF}_6]^{3+}$, 610 (23) $[M-4\text{PF}_6]^{4+}$; elemental analysis calcd (%) for $\text{C}_{158}\text{H}_{166}\text{F}_{24}\text{N}_4\text{O}_{12}\text{P}_4\text{S}_4$ (3024): C 62.81, H 5.54, N 1.85; found: C 62.55, H 5.57, N 1.81; UV/Vis (MeCN): $\lambda_{\text{max}}=846$ nm, $\epsilon=3700$ L mol⁻¹ cm⁻¹.

Compound 25: PPh_3 (2.16 g, 8.24 mmol) was added in portions during 15 min to a stirred solution of compound **24**^[25] (2.52 g, 7.49 mmol) and CBr_4 (2.74 g, 8.26 mmol) in dry THF (25 mL) at room temperature. The reaction mixture was stirred for 2 h and then Et_2O (50 mL) was added. The mixture was filtered and concentrated in vacuo to give a brown oil which was then subjected to column chromatography (silica gel: $\text{CH}_2\text{Cl}_2/\text{MeOH}$ 24:1) to afford compound **25** (1.04 g, 35%) as a white solid. M.p. 79–81 °C; ^1H NMR (CDCl_3 , 200 MHz): $\delta=2.20$ (s, 1H), 3.52 (t, $J=6.2$ Hz, 2H), 3.69–3.80 (m, 4H), 3.92–4.03 (m, 6H), 4.27–4.31 (m, 4H),

6.84 (d, $J=8.0$, 2H), 7.37 (t, $J=8.0$ Hz, 2H), 7.88 (d, $J=8.0$ Hz, 2H); ^{13}C NMR (CDCl_3 , 50 MHz): $\delta=30.5$, 61.9, 61.9, 68.0, 69.8, 69.8, 71.5, 72.7, 105.9, 105.9, 114.7, 114.8, 125.2, 125.3, 126.8, 126.8, 154.3, 154.3; MS (FAB): m/z (%): 401 (58) $[\text{M}+\text{H}+2]^+$, 400 (100) $[\text{M}+2]^+$, 399 (61) $[\text{M}+\text{H}]^+$, 398 (96) $[\text{M}]^+$; elemental analysis calcd (%) for $\text{C}_{18}\text{H}_{23}\text{O}_5\text{Br}$ (399): C 54.15, H 5.81; found: C 53.91, H 5.71.

Compound 26: A solution of compound **25** (4.07 g, 10.2 mmol) *tert*-butylchlorodimethyl silane (1.95 g, 13 mmol) and imidazole (0.88 g, 13 mmol) in anhydrous DMF (20 mL) was stirred at room temperature for 16 h. The reaction mixture was then poured into H_2O (20 mL) and extracted with Et_2O (3×200 mL). The combined organic layers were washed with H_2O and brine, and dried (MgSO_4). The solvent was evaporated in vacuo to give a crude product as a yellow oil, which was purified by column chromatography (silica gel: CH_2Cl_2 /hexanes 1:9) to yield compound **26** (5.19 g, 99%) as a colorless oil. ^1H NMR (CDCl_3 , 500 MHz): $\delta=0.09$ (s, 6H), 0.92 (s, 9H), 3.51 (t, $J=6.2$ Hz, 2H), 3.71 (t, $J=5.2$ Hz, 2H), 3.82 (t, $J=5.2$ Hz, 2H), 3.95 (t, $J=6.2$ Hz, 2H), 3.97–4.02 (m, 4H), 4.26–4.30 (m, 4H), 6.84 (d, $J=8.0$, 1H), 6.84 (d, $J=8.0$, 1H), 7.35 (t, $J=8.0$ Hz, 1H), 7.35 (t, $J=8.0$ Hz, 1H), 7.87 (d, $J=8.0$ Hz, 1H), 7.90 (d, $J=8.0$ Hz, 1H); ^{13}C NMR (CDCl_3 , 125 MHz): $\delta=-5.3$, 18.3, 25.9, 30.3, 62.8, 67.8, 67.9, 69.6, 69.8, 71.4, 72.9, 105.6, 105.6, 114.4, 114.8, 124.9, 125.0, 126.6, 126.7, 154.0, 154.3; MS (FAB): m/z (%): 514 (70) $[\text{M}+2]^+$, 513 (100) $[\text{M}+\text{H}]^+$, 512 (61) $[\text{M}]^+$; HRMS (FAB): calcd for $\text{C}_{22}\text{H}_{37}\text{BrO}_5\text{Si}$: 512.1594; found: 512.1597.

Compound 27: A solution of compound **26** (1.60 g, 3.11 mmol), K_2CO_3 (0.85 g, 6.22 mmol), 4-bromo-(1,1'-biphenyl)-4-ol (**16**) (1.16 g, 4.66 mmol), and [18]crown-6 (20 mg, cat. amount) in dry MeCN (20 mL) was heated under reflux for 16 h. After cooling down to room temperature, the reaction mixture was filtered and the solid was washed with CH_2Cl_2 (100 mL). The combined organic solution was concentrated and the residue was purified by column chromatography (silica gel: CH_2Cl_2) to afford compound **27** (1.31 g, 62%) as an off-white powder. M.p. 89–91 °C; ^1H NMR (CD_3COCD_3 , 500 MHz): $\delta=0.07$ (s, 6H), 0.90 (s, 9H), 3.71 (t, $J=5.3$ Hz, 2H), 3.82 (t, $J=5.3$ Hz, 2H), 4.00 (t, $J=5.0$ Hz, 2H), 4.03 (t, $J=4.8$ Hz, 2H), 4.09 (t, $J=4.8$ Hz, 2H), 4.22 (t, $J=4.8$ Hz, 2H), 4.27 (t, $J=5.0$ Hz, 2H), 4.34 (t, $J=4.8$ Hz, 2H), 6.83 (d, $J=6.8$ Hz, 1H), 6.85 (d, $J=6.8$ Hz, 1H), 6.98 (d, $J=8.8$ Hz, 2H), 7.32 (dd, $J=6.8$, 9.1 Hz, 1H), 7.34 (dd, $J=6.8$, 9.1 Hz, 1H), 7.40 (d, $J=8.5$ Hz, 2H), 7.46 (d, $J=8.8$ Hz, 2H), 7.52 (d, $J=8.5$ Hz, 2H), 7.86 (d, $J=9.1$ Hz, 1H), 6.83 (d, $J=9.1$ Hz, 1H); ^{13}C NMR (CDCl_3 , 125 MHz): $\delta=-5.2$, 18.4, 25.9, 62.9, 67.7, 68.0, 68.0, 69.9, 70.0, 73.0, 105.6, 105.7, 114.5, 114.8, 115.1, 120.8, 125.0, 125.1, 126.8, 126.8, 127.9, 128.3, 131.8, 132.7, 139.7, 154.3, 154.4, 158.6; MS (FAB): m/z (%): 683 (80) $[\text{M}+\text{H}]^+$, 682 (100) $[\text{M}]^+$, 681 (84) $[\text{M}-\text{H}]^+$; HRMS (MALDI-TOF): calcd for $\text{C}_{36}\text{H}_{45}\text{BrO}_6\text{SiNa}$: 703.2067; found: 703.2061.

Compound 29: A solution of the Grignard reagent **19** (5 mL, 5 mmol) was added to a solution of compound **27** (1.93 g, 2.83 mmol) and $\text{Pd}(\text{PPh}_3)_4$ (0.16 g, cat. amount) in anhydrous THF (10 mL), and the mixture was heated under reflux for 16 h. After cooling down to room temperature, the solvent was evaporated yielding a yellow powder, which was dissolved in CH_2Cl_2 (25 mL). Trifluoroacetic acid (0.5 g, cat. amount) was added to this mixture and it was stirred at room temperature for another 16 h, whereupon the mixture was poured into H_2O (50 mL), extracted with CHCl_3 and dried (MgSO_4). The combined organic layers were concentrated and the residue was subjected to column chromatography (silica gel: EtOAc /hexanes 1:2) to yield compound **29** (1.58 g, 71%) as a white powder. M.p. 166–168 °C; ^1H NMR (CD_3COCD_3 , 500 MHz): $\delta=3.57$ (brs, 1H), 3.64–3.66 (m, 4H), 3.94 (t, $J=4.7$ Hz, 2H), 3.98 (t, $J=4.7$ Hz, 2H), 4.05 (t, $J=4.7$ Hz, 2H), 4.23 (t, $J=4.7$ Hz, 2H), 4.27 (t, $J=4.7$ Hz, 2H), 4.33 (t, $J=4.7$ Hz, 2H), 6.91 (d, $J=4.7$ Hz, 2H), 6.91 (d, $J=8.6$ Hz, 2H), 6.94 (d, $J=8.7$ Hz, 1H), 6.97 (d, $J=7.6$ Hz, 1H), 7.03 (d, $J=8.6$ Hz, 2H), 7.33 (dd, $J=4.7$, 9.0 Hz, 1H), 7.34 (dd, $J=4.7$, 9.0 Hz, 1H), 7.53 (d, $J=8.6$ Hz, 2H), 7.59 (d, $J=8.7$ Hz, 2H), 7.81 (d, $J=9.0$ Hz, 1H), 7.83 (d, $J=9.0$ Hz, 1H), 8.42 (s, 1H); MS (FAB): m/z (%): 580 (100) $[\text{M}]^+$; elemental analysis calcd (%) for $\text{C}_{36}\text{H}_{36}\text{O}_7$ (580): C 74.46, H 6.25; found: C 74.11, H 6.29.

Half-dumbbell-shaped compound 30: A solution of compound **14** (842 mg, 0.80 mmol), compound **29** (465 mg, 0.8 mmol), K_2CO_3 (484 mg, 4.0 mol), LiBr (10 mg, cat. amount) and [18]crown-6 (10 mg, cat. amount) in anhydrous MeCN (10 mL) was heated under reflux for 16 h. After cooling down to room temperature, the reaction mixture was filtered and

the solid was washed with Me_2CO (30 mL). The combined organic solution was concentrated and the residue was purified by column chromatography (silica gel: CH_2Cl_2 /EtOH 100:3) to give the half-dumbbell-shaped compound **30** (664 mg, 82%) as a yellow powder. M.p. 115–117 °C; ^1H NMR (CDCl_3 , 400 MHz): $\delta=1.22$ (t, $J=7.5$ Hz, 3H), 1.29 (s, 18H), 2.10 (t, $J=5.8$ Hz, 1H), 2.61 (q, $J=7.5$ Hz, 2H), 3.59–3.63 (m, 4H), 3.70–3.79 (m, 8H), 3.80–3.85 (m, 2H), 3.88–3.93 (m, 2H), 4.00–4.08 (m, 4H), 4.08–4.14 (m, 4H), 4.17–4.25 (m, 4H), 4.27–4.37 (m, 8H), 6.20, 6.21 (2×s, 2H), 6.76 (d, $J=8.7$ Hz, 2H), 6.86 (d, $J=8.7$ Hz, 2H), 6.97–7.11 (m, 14H), 7.23 (d, $J=8.5$ Hz, 4H), 7.31–7.42 (m, 2H), 7.50–7.63 (m, 8H), 7.85 (d, $J=9.0$ Hz, 2H); ^{13}C NMR (CDCl_3 , 100 MHz): $\delta=15.1$, 28.2, 29.6, 31.2, 34.2, 61.4, 63.1, 67.5, 67.6, 67.6, 67.9, 67.9, 68.1, 68.2, 68.3, 69.2, 69.3, 69.5, 70.0, 70.2, 70.5, 72.6, 105.6, 113.1, 114.6, 114.7, 116.0, 116.6, 116.6, 124.0, 125.0, 126.4, 126.8, 126.8, 127.8, 130.2, 130.5, 133.4, 134.2, 134.3, 134.4, 134.4, 139.0, 139.7, 141.7, 143.2, 144.9, 147.3, 154.2, 156.4, 158.1; MS(FAB): m/z (%): 1460 (100) $[\text{M}]^+$; HRMS (FAB): calcd for $\text{C}_{87}\text{H}_{96}\text{O}_{12}\text{S}_4$: 1460.5785; found: 1460.5785.

Dumbbell-shaped compound 4: A solution of compound **30** (100 mg, 0.07 mmol), the dendritic chloride **31** (109 mg, 0.14 mmol), NaH (48 mg, 2.0 mol), NaI (10 mg, cat. amount) and [15]crown-5 (10 mg, cat. amount) in anhydrous THF (10 mL) was heated under reflux for 16 h. After cooling down to room temperature, MeOH (1 mL) was added to the reaction mixture. The solvent was evaporated and the residue was purified by column chromatography (silica gel: $\text{EtOAc}/\text{CH}_2\text{Cl}_2$ 1:2) to give the dumbbell-shaped compound **4** (80 mg, 51%) as a yellow powder. M.p. 65–68 °C; ^1H NMR (CD_3COCD_3 , 500 MHz): $\delta=1.20$ (t, $J=7.5$ Hz, 3H), 1.30 (s, 18H), 2.57 (q, $J=7.5$ Hz, 2H), 3.28 (s, 6H), 3.29 (s, 3H), 3.47–3.51 (m, 6H), 3.59–3.70 (m, 16H), 3.75–3.80 (m, 10H), 3.81–3.83 (m, 2H), 3.97 (t, $J=4.7$ Hz, 4H), 4.03 (t, $J=4.7$ Hz, 2H), 4.08–4.14 (m, 8H), 4.18–4.21 (m, 2H), 4.23 (t, $J=4.7$ Hz, 2H), 4.28–4.32 (m, 8H), 4.47 (s, 2H), 4.90 (s, 2H), 4.98 (s, 4H), 6.32, 6.44, 6.59 (3×s, 2H), 6.73 (s, 2H), 6.78–6.85 (m, 4H), 6.91–6.96 (m, 6H), 7.00–7.04 (m, 4H), 7.04–7.14 (m, 10H), 7.25–7.35 (m, 12H), 7.55–7.65 (m, 8H), 7.85 (d, $J=8.2$ Hz, 1H), 7.87 (d, $J=8.2$ Hz, 1H); ^{13}C NMR (CD_3COCD_3 , 125 MHz): $\delta=14.6$, 27.7, 29.1, 30.6, 33.8, 57.8, 63.1, 67.5, 67.5, 67.5, 67.6, 67.6, 67.7, 68.1, 69.3, 69.4, 69.5, 69.5, 69.6, 69.6, 70.3, 70.4, 70.4, 70.7, 71.7, 72.5, 74.2, 105.9, 105.9, 107.2, 107.2, 113.3, 114.0, 114.3, 114.4, 115.0, 116.1, 116.2, 123.9, 124.9, 126.5, 126.6, 126.6, 126.9, 127.5, 127.6, 129.1, 129.7, 129.7, 130.5, 130.7, 131.8, 132.9, 134.1, 134.3, 134.7, 134.9, 137.8, 138.8, 139.4, 141.3, 144.3, 144.6, 148.2, 152.8, 154.4, 157.0, 158.7, 158.8; MS(FAB): m/z (%): 2224 (70) $[\text{M}]^+$, 1460 (100); elemental analysis calcd (%) for $\text{C}_{130}\text{H}_{150}\text{O}_{24}\text{S}_4$: C 70.18, H 6.79; found: C 69.88, H 6.87.

[2]Rotaxane 3-4PF₆: A solution of dumbbell-shaped compound **4** (200 mg, 0.10 mmol), the dicationic salt **22-2PF₆** (212 mg, 0.30 mmol) and α,α' -dibromo-*p*-xylene (**23**) (79 mg, 0.30 mmol) in anhydrous DMF (10 mL) was stirred for 10 d at room temperature (after approximately 2 d, the color changed to dark green and a white precipitate formed). The green suspension was subjected to column chromatography (silica gel) and the unreacted compound **4** was eluted with Me_2CO . Thereafter, the eluent was changed to $\text{Me}_2\text{CO}/\text{NH}_4\text{PF}_6$ (1.0 g NH_4PF_6 in 100 mL Me_2CO) and a green band containing the rotaxane **3-4PF₆** was collected. Most of the solvent was removed under vacuum. After adding H_2O (50 mL) to the residue, the precipitate was collected by filtration, washed with Et_2O (30 mL), and dried in vacuo to afford the rotaxane **3-4PF₆** (210 mg, 60%) as a green powder. M.p. 115 °C (decomposed without melting); ^1H NMR (CD_3CN , 500 MHz): $\delta=1.18$ (2×t, $J=7.5$ Hz, 3H), 1.26–1.30 (m, 18H), 2.57 (q, $J=7.5$ Hz, 2H), 3.26 (s, 9H), 3.45–3.48 (m, 6H), 3.57–3.61 (m, 6H), 3.71–3.80 (m, 8H), 3.85–4.28 (m, 40H), 4.42 (s, 2H), 4.78 (s, 2H), 4.89 (s, 4H), 5.43–5.70 (m, 8H), 6.03, 6.11, 6.22, 6.28 (4×s, 2H), 6.50 (d, $J=6.8$ Hz, 1H), 6.55 (d, $J=6.8$ Hz, 1H), 6.60–6.70 (m, 4H), 6.71–6.94 (m, 6H), 6.96–7.12 (m, 14H), 7.14–7.37 (m, 16H), 7.42–7.62 (m, 14H), 7.64–7.82 (m, 8H), 8.84–9.01 (m, 8H); MS (FAB): m/z : 3179 $[\text{M}-\text{PF}_6]^+$, 3034 $[\text{M}-2\text{PF}_6]^+$, 2888 $[\text{M}-3\text{PF}_6]^+$, 1517 $[\text{M}-2\text{PF}_6]^{2+}$, 1445 $[\text{M}-3\text{PF}_6]^{2+}$, 1372 $[\text{M}-4\text{PF}_6]^{2+}$; elemental analysis calcd (%) for $\text{C}_{166}\text{H}_{182}\text{F}_{24}\text{N}_4\text{O}_{24}\text{P}_4\text{S}_4$ (3324): C 59.96, H 5.52, N 1.68; found: C 59.69, H 5.43, N 1.65; UV/Vis (MeCN): $\lambda_{\text{max}}=846$ nm, $\epsilon=2900$ $\text{L mol}^{-1} \text{cm}^{-1}$.

Half-dumbbell-shaped compound 32: A solution of compound **21** (519 mg, 0.50 mmol), compound **11** (297 mg, 0.50 mmol), K_2CO_3 (267 mg, 2.0 mol), LiBr (10 mg, cat. amount) and [18]crown-6 (10 mg, cat. amount) in anhydrous MeCN (10 mL) was heated under reflux for 16 h. After

cooling, the reaction mixture was filtered and the solid was washed with Me₂CO. The combined organic solution was concentrated, and the residue was purified by column chromatography (silica gel: CH₂Cl₂/EtOH 100:3) to give the half-dumbbell-shaped compound **32** (467 mg, 64%) as a yellow powder. M.p. 106–108 °C; ¹H NMR (CDCl₃, 400 MHz): δ = 1.23 (t, *J* = 7.6 Hz, 3H), 1.30 (s, 18H), 2.15 (brs, 1H), 2.62 (q, *J* = 7.5 Hz, 2H), 3.58–3.63 (m, 4H), 3.64–3.68 (m, 4H), 3.72–3.77 (m, 4H), 3.89 (t, *J* = 4.4 Hz, 2H), 3.98 (t, *J* = 4.8 Hz, 2H), 4.04 (t, *J* = 4.8 Hz, 2H), 4.06 (t, *J* = 4.9 Hz, 2H), 4.09 (t, *J* = 4.8 Hz, 2H), 4.15 (t, *J* = 4.8 Hz, 2H), 4.20 (t, *J* = 4.8 Hz, 2H), 4.23 (t, *J* = 4.8 Hz, 2H), 4.28 (s, 2H), 4.30 (s, 2H), 4.31–4.34 (m, 4H), 6.19, 6.20 (2 × s, 2H), 6.76 (d, *J* = 8.9 Hz, 2H), 6.84 (d, *J* = 8.7 Hz, 2H), 7.01 (d, *J* = 8.8 Hz, 2H), 7.02 (d, *J* = 8.9 Hz, 2H), 7.03–7.10 (m, 10H), 7.22 (d, *J* = 8.5 Hz, 4H), 7.31 (t, *J* = 8.7 Hz, 1H), 7.32 (t, *J* = 8.7 Hz, 1H), 7.54 (d, *J* = 8.8 Hz, 2H), 7.56 (d, *J* = 8.8 Hz, 2H), 7.60 (s, 4H), 7.86 (d, *J* = 8.70 Hz, 1H), 7.87 (d, *J* = 8.7 Hz, 1H); ¹³C NMR (CDCl₃, 125 MHz): δ = 15.2, 28.1, 29.6, 31.3, 34.2, 61.7, 63.0, 67.2, 67.4, 67.6, 67.9, 67.9, 68.1, 68.2, 68.2, 69.1, 69.2, 69.2, 69.3, 69.8, 69.9, 70.0, 70.2, 70.7, 72.3, 105.6, 113.1, 114.5, 114.6, 114.9, 114.9, 116.2, 116.3, 116.5, 124.0, 125.0, 126.5, 126.7, 126.9, 127.8, 130.6, 130.9, 132.1, 133.4, 134.2, 134.3, 134.4, 134.4, 139.0, 139.7, 141.3, 144.0, 144.5, 148.2, 154.2, 154.2, 156.4, 158.2; MS (FAB): *m/z* (%): 1460 (100) [M]⁺; HRMS (MALDI-TOF): calcd for C₈₇H₉₆O₁₂S₄Na: 1483.5682; found: 1483.5684.

Dumbbell-shaped compound 6: A solution of compound **32** (350 mg, 0.24 mmol), the dendritic chloride **31** (278 mg, 0.35 mmol), NaH (18 mg, 0.75 mol), NaI (10 mg, cat. amount) and [15]crown-5 (10 mg, cat. amount) in anhydrous THF (20 mL) was heated under reflux for 16 h. After the reaction had been cooled down to room temperature, the solvent was evaporated and the residue was purified by column chromatography (silica gel: EtOH/CH₂Cl₂ 2:100) to give the dumbbell-shaped compound **6** (352 mg, 66%) as a yellow powder. M.p. 78–80 °C; ¹H NMR (CD₃COCD₃, 500 MHz): δ = 1.18 (t, *J* = 7.5 Hz, 3H), 1.27 (s, 18H), 2.57 (q, *J* = 7.5 Hz, 2H), 3.27 (s, 9H), 3.47 (t, *J* = 4.8 Hz, 6H), 3.55–3.68 (m, 16H), 3.74–3.81 (m, 8H), 3.92 (t, *J* = 4.8 Hz, 2H), 3.95 (t, *J* = 4.8 Hz, 2H), 3.99 (t, *J* = 4.8 Hz, 2H), 4.01 (t, *J* = 4.8 Hz, 2H), 4.08 (t, *J* = 4.8 Hz, 2H), 4.08–4.16 (m, 8H), 4.20 (t, *J* = 4.8 Hz, 2H), 4.26 (s, 2H), 4.28–4.32 (m, 8H), 4.43 (s, 2H), 4.90 (s, 2H), 5.01 (s, 4H), 6.39, 6.40, 6.41, 6.43 (4 × s, 2H), 6.73 (s, 2H), 6.78–6.81 (m, 4H), 6.91–6.94 (m, 6H), 6.98–7.02 (m, 4H), 7.04–7.14 (m, 10H), 7.23–7.31 (m, 8H), 7.36 (d, *J* = 8.3 Hz, 4H), 7.53–7.64 (m, 8H), 7.82 (d, *J* = 8.3 Hz, 1H), 7.84 (d, *J* = 8.3 Hz, 1H); ¹³C NMR (CD₃COCD₃, 125 MHz): δ = 14.6, 27.7, 29.1, 30.6, 33.8, 57.8, 63.1, 67.5, 67.5, 67.5, 67.6, 67.7, 68.1, 69.3, 69.4, 69.5, 69.5, 69.6, 69.6, 70.3, 70.4, 70.4, 70.7, 71.7, 72.5, 74.2, 105.9, 105.9, 107.2, 107.2, 113.3, 114.0, 114.3, 114.4, 115.0, 116.1, 116.2, 123.9, 124.9, 126.5, 126.6, 126.6, 126.9, 127.5, 127.6, 129.1, 129.7, 129.7, 130.5, 130.7, 131.8, 132.9, 134.1, 134.3, 134.7, 134.9, 137.8, 138.8, 139.4, 141.3, 144.3, 144.6, 148.2, 152.8, 154.4, 157.0, 158.7, 158.8; MS (FAB): *m/z* (%): 2224 (100) [M]⁺, 1460 (50); elemental analysis calcd (%) for C₁₃₀H₁₅₀O₂₄S₄ (2224): C 70.18, H 6.79; found C 69.96, H 6.81.

[2]Rotaxane 5-4PF₆: A solution of dumbbell-shaped compound **6** (320 mg, 0.14 mmol), the dicationic salt **22-2PF₆** (304 mg, 0.43 mmol) and α,α'-dibromo-*p*-xylene (**23**) (114 mg, 0.43 mmol) in anhydrous DMF (20 mL) was stirred for 10 d at room temperature (after approximately 2 d the color changed to dark green and a white precipitate formed). The green suspension was subjected to column chromatography (silica gel) and unreacted compound **6** was eluted with Me₂CO, whereupon the eluent was changed to Me₂CO/NH₄PF₆ (1.0 g NH₄PF₆ in 100 mL Me₂CO) and a green band containing the rotaxane **5-4PF₆** was collected. Most of the solvent was removed under vacuum. After adding H₂O (50 mL) to the residue, the precipitate was collected by filtration, washed with Et₂O (30 mL), and dried in vacuo to afford the rotaxane **5-4PF₆** (265 mg, 57%) as a green powder. M.p. 185–187 °C; ¹H NMR (CD₃CN, 500 MHz): δ = 1.20 (t, *J* = 7.6 Hz, 3H), 1.29 (s, 18H), 2.61 (q, *J* = 7.5 Hz, 2H), 3.30 (s, 6H), 3.31 (s, 3H), 3.50–3.52 (m, 6H), 3.63–3.65 (m, 6H), 3.79–3.83 (m, 10H), 3.84–3.93 (m, 8H), 3.97–3.99 (m, 6H), 4.02–4.19 (m, 16H), 4.26–4.32 (m, 10H), 4.79 (s, 2H), 4.81 (s, 2H), 4.83 (s, 2H), 5.38–5.64 (m, 8H), 5.97, 6.03, 6.16, 6.24 (4 × s, 2H), 6.47 (d, *J* = 8.4 Hz, 2H), 6.76–6.87 (m, 6H), 6.92–6.96 (m, 6H), 7.03 (d, *J* = 8.8 Hz, 1H), 7.04 (d, *J* = 8.8 Hz, 1H), 7.10–7.17 (m, 10H), 7.24 (d, *J* = 8.4 Hz, 4H), 7.29–7.37 (m, 8H), 7.48 (d, *J* = 8.8 Hz, 1H), 7.49 (d, *J* = 8.8 Hz, 1H), 7.53–7.67 (m, 18H), 7.69–7.74 (m, 4H), 7.81 (d, *J* = 8.8 Hz, 1H), 7.83 (d, *J* = 8.8 Hz, 1H), 8.65–8.95 (m, 8H); MS (FAB): *m/z*: 3178 [M–PF₆]⁺, 3035 [M–2PF₆]⁺, 2888

[M–3PF₆]⁺, 1517 [M–2PF₆]²⁺, 1446 [M–3PF₆]²⁺, 1372 [M–4PF₆]²⁺; elemental analysis calcd (%) for C₁₆₆H₁₈₂F₂₄N₄O₂₄P₄S₄: C 59.96, H 5.52, N 1.68; found: C 59.74, H 5.55, N 1.65; UV/Vis (MeCN): λ_{max} = 850 nm, ε = 4200 L mol⁻¹ cm⁻¹.

Photophysical experiments: All the measurements were performed at room temperature in air-equilibrated MeCN solutions (2 × 10⁻⁵–1 × 10⁻⁴ M). UV/Vis absorption spectra were recorded with a Perkin-Elmer Lambda 40 spectrophotometer. Uncorrected fluorescence spectra were obtained with a Perkin-Elmer LS-50 spectrofluorimeter equipped with a Hamamatsu R928 phototube. The estimated experimental errors are: 2 nm on band maxima, ±5% on the molar absorption coefficients and fluorescence intensity. The emission quantum yield of the *p*-dimethoxyterphenyl spacer was obtained using 1,5-dimethoxynaphthalene as a reference (φ_{em} = 0.38 in aerated MeCN solution).^[49] An Edinburgh 199 single-photon counting apparatus was used for lifetime measurements. The experimental error on the lifetime values is estimated to be ±10%.

Electrochemical experiments: Cyclic voltammetric (CV) and differential pulse voltammetric (DPV) experiments were carried out in argon-purged MeCN solution at room temperature with an Autolab 30 multipurpose instrument interfaced to a personal computer. The working electrode was a glassy carbon electrode (0.08 cm², Amel); its surface was routinely polished with 0.05 mm alumina/water slurry on a felt surface, immediately prior to use. In all cases, the counter electrode was a Pt spiral, separated from the bulk solution with a fine glass frit, and an Ag wire was used as a quasi-reference electrode. 1,1-Dimethylferrocene^[50] (+0.30 V vs SCE) was present as an internal standard for all rotaxanes. For the dumbbells, because of peak overlapping problems, it was more convenient to use decamethylferrocene^[51] as internal standard (–0.11 V vs SCE). The concentrations of the compounds were in the range 1 × 10⁻⁴–5 × 10⁻⁴ M; the experiments were carried out in the presence of 0.05 M tetraethylammonium hexafluorophosphate as supporting electrolyte. Cyclic voltammograms were obtained with sweep rates in the range 0.05–1.0 V s⁻¹; the DPV experiments were performed with a scan rate of 20 or 4 mV s⁻¹ (pulse height 75 and 10 mV, respectively) and a duration of 40 ms. The reversibility of the observed processes was established by using the criteria of i) separation of 60 mV between cathodic and anodic peaks, ii) the close to unity ratio of the intensities of the cathodic and anodic currents, and iii) the constancy of the peak potential on changing sweep rate in the cyclic voltammograms. The same halfwave potential values were obtained from the DPV peaks and from an average of the cathodic and anodic CV peaks, as expected for reversible processes. For irreversible processes the potential values were estimated from the DPV peaks. The number of exchanged electrons in the redox processes of the investigated dumbbells and rotaxanes was measured by comparing the current intensity of the CV waves and the area of the DPV peaks with those found for the two reversible and bi-electronic reduction processes of the cyclophane^[21a,33,39] **36⁴⁺** after correction for differences in concentration and diffusion coefficients.^[52] The fitting and deconvolution of the DPV peaks were obtained by employing the equations proposed by Parry and Osteryoung.^[53] The experimental error on the potential values was estimated to be ±10 mV and ±20 mV for reversible and irreversible processes, respectively.

Chemical redox experiments: Titration with a standardized Fe(ClO₄)₃ solution was performed in MeCN solution at room temperature. The concentration of [2]rotaxane solution was 2.0 × 10⁻⁵ M. In the NMR spectroscopic experiments, 2.2 equivalents of the oxidant, tris(*p*-bromophenyl)ammonium hexafluoroantimonate,^[23] were added to a 1 mM solution of **5-4PF₆** in CD₃CN at 243 K.

Acknowledgement

This research was supported at the University of California at Los Angeles by the Defense Advanced Research Projects Agency (DARPA). Some of the compound characterizations were supported by the National Science Foundation under equipment grant no CHE-9974928. In Italy, this research was supported by the European Community (HPRN-CT-2000-00029 project), the University of Bologna (Funds for Selected Research Topics) and MIUR (Supramolecular Devices Project). In Den-

mark, this research was supported by Carlsbergfondet and the Familien Hede Nielsen Fond.

- [1] a) J.-M. Lehn, *Supramolecular Chemistry*, VCH, Weinheim, **1995**; b) *Comprehensive Supramolecular Chemistry* (Eds.: J.-M. Lehn, J. L. Atwood, J. E. D. Davies, D. D. MacNicol, F. Vögtle), Pergamon, Oxford, **1996**; c) H.-J. Schneider, A. Yatsimirsky, *Principles and Methods in Supramolecular Chemistry*, Wiley-VCH, Weinheim, **2000**; d) J. W. Steed, J. L. Atwood, *Supramolecular Chemistry*, Wiley-VCH, Weinheim, **2000**; e) J.-M. Lehn, *Science* **2002**, *295*, 2400–2403; f) O. Ikkala, G. ten Brinke, *Science* **2002**, *295*, 2407–2409; g) M. D. Hollingsworth, *Science* **2002**, *295*, 2410–2413; h) T. Kato, *Science* **2002**, *295*, 2414–2418; i) G. M. Whitesides, B. Grzybowski, *Science* **2002**, *295*, 2418–2421.
- [2] a) J. S. Lindsey, *New J. Chem.* **1991**, *15*, 153–180; b) G. M. Whitesides, J. P. Mathias, C. T. Seto, *Science* **1991**, *254*, 1312–1319; c) D. Philp, J. F. Stoddart, *Synlett* **1991**, 445–458; d) M. Fujita, *Acc. Chem. Res.* **1999**, *32*, 53–61; e) J. Rebek, Jr., *Acc. Chem. Res.* **1999**, *32*, 278–286; f) D. T. Bong, T. D. Clark, J. R. Granja, M. R. Ghadiri, *Angew. Chem.* **2001**, *113*, 1016–1041; *Angew. Chem. Int. Ed.* **2001**, *40*, 988–1011; g) L. J. Prins, D. N. Reinhoudt, P. Timmerman, *Angew. Chem.* **2001**, *113*, 2446–2492; *Angew. Chem. Int. Ed.* **2001**, *40*, 2382–2426; h) S. R. Seidel, P. J. Stang, *Acc. Chem. Res.* **2002**, *35*, 972–983.
- [3] a) D. N. Reinhoudt, M. Crego-Calama, *Science* **2002**, *295*, 2403–2407.
- [4] a) S. Anderson, H. L. Anderson, J. K. M. Sanders, *Acc. Chem. Res.* **1993**, *26*, 469–475; b) J. P. Schneider, J. W. Kelly, *Chem. Rev.* **1995**, *95*, 2169–2187; c) F. M. Raymo, J. F. Stoddart, *Pure Appl. Chem.* **1996**, *68*, 313–322; d) *Templated Organic Synthesis* (Eds.: F. Diederich, P. J. Stang), Wiley-VCH, Weinheim, **1999**; e) J. F. Stoddart, H.-R. Tseng, *Proc. Natl. Acad. Sci. USA* **2002**, *99*, 4797–4800.
- [5] a) G. Schill, *Catenanes, Rotaxanes, and Knots*, Academic Press, New York, **1971**; b) *Molecular Catenanes, Rotaxanes and Knots* (Eds.: J.-P. Sauvage, C. O. Dietrich-Buchecker), Wiley-VCH, Weinheim, **1999**.
- [6] a) P.-L. Anelli, N. Spencer, J. F. Stoddart, *J. Am. Chem. Soc.* **1991**, *113*, 5131–5133; b) P.-L. Anelli, M. Asakawa, P. R. Ashton, R. A. Bissell, G. Clavier, R. Górski, A. E. Kaifer, S. J. Langford, G. Matternsteig, S. Menzer, D. Philp, A. M. Z. Slawin, N. Spencer, J. F. Stoddart, M. S. Tolley, D. J. Williams, *Chem. Eur. J.* **1997**, *3*, 1113–1135; c) D. A. Leigh, A. Troisi, F. Zerbetto, *Angew. Chem.* **2000**, *112*, 358–361; *Angew. Chem. Int. Ed.* **2000**, *39*, 350–353; d) J. Cao, M. C. T. Fyfe, J. F. Stoddart, G. R. L. Cousins, P. T. Glink, *J. Org. Chem.* **2000**, *65*, 1937–1946; e) A. M. Elizarov, T. Chang, S.-H. Chiu, J. F. Stoddart, *Org. Lett.* **2002**, *4*, 3565–3568.
- [7] a) G. Schill, K. Rissler, H. Fritz, W. Vetter, *Angew. Chem.* **1981**, *93*, 197–201; *Angew. Chem. Int. Ed. Engl.* **1981**, *20*, 187–189.
- [8] a) M. C. T. Fyfe, P. T. Glink, S. Menzer, J. F. Stoddart, A. J. P. White, D. J. Williams, *Angew. Chem.* **1997**, *109*, 2158–2160; *Angew. Chem. Int. Ed. Engl.* **1997**, *36*, 2068–2070; b) M. C. T. Fyfe, J. F. Stoddart, *Acc. Chem. Res.* **1997**, *30*, 393–401.
- [9] a) P. R. Ashton, R. A. Bissell, N. Spencer, J. F. Stoddart, M. S. Tolley, *Synlett* **1992**, 923–926; b) E. Córdova, R. A. Bissell, N. Spencer, P. R. Ashton, A. E. Kaifer, J. F. Stoddart, *J. Org. Chem.* **1993**, *58*, 6550–6552; c) W. Devonport, M. A. Blower, M. R. Bryce, L. M. Goldenberg, *J. Org. Chem.* **1997**, *62*, 885–887; d) P. R. Ashton, R. Ballardini, V. Balzani, M. Gómez-López, S. E. Lawrence, M.-V. Martínez-Díaz, M. Montalti, A. Piersanti, L. Prodi, J. F. Stoddart, D. J. Williams, *J. Am. Chem. Soc.* **1997**, *119*, 10641–10651; e) P. R. Ashton, R. Ballardini, V. Balzani, I. Baxter, A. Credi, M. C. T. Fyfe, M. T. Gandolfi, M. Gómez-López, M.-V. Martínez-Díaz, A. Piersanti, N. Spencer, J. F. Stoddart, M. Venturi, A. J. P. White, D. J. Williams, *J. Am. Chem. Soc.* **1998**, *120*, 11932–11942; f) A. M. Elizarov, H.-S. Chiu, J. F. Stoddart, *J. Org. Chem.* **2002**, *67*, 9175–9181.
- [10] a) R. A. Bissell, E. Córdova, A. E. Kaifer, J. F. Stoddart, *Nature* **1994**, *369*, 133–137; b) L. Raehm, J.-M. Kern, J.-P. Sauvage, *Chem. Eur. J.* **1999**, *5*, 3310–3317; c) R. Ballardini, V. Balzani, W. Dehaen, A. E. Dell'Erba, F. M. Raymo, J. F. Stoddart, M. Venturi, *Eur. J. Org. Chem.* **2000**, 591–602; d) J.-P. Collin, J.-M. Kern, L. Raehm, J.-P. Sauvage in *Molecular Switches* (Ed.: B. L. Feringa), Wiley-VCH, Weinheim, **2000**, p. 249–280; e) B. X. Colasson, C. Dietrich-Buchecker, M. C. Jimenez-Molero, J.-P. Sauvage, *J. Phys. Org. Chem.* **2002**, *15*, 476–483.
- [11] a) C. P. Collier, G. Matternsteig, E. W. Wong, Y. Luo, K. Beverly, J. Sampaio, F. M. Raymo, J. F. Stoddart, J. R. Heath, *Science* **2000**, *289*, 1172–1175; b) A. R. Pease, J. O. Jeppesen, J. F. Stoddart, Y. Luo, C. P. Collier, J. R. Heath, *Acc. Chem. Res.* **2001**, *34*, 433–444; c) C. P. Collier, J. O. Jeppesen, Y. Luo, J. Perkins, E. W. Wong, J. R. Heath, J. F. Stoddart, *J. Am. Chem. Soc.* **2001**, *123*, 12632–12641; d) Y. Luo, C. P. Collier, J. O. Jeppesen, K. A. Nielsen, E. Delonno, G. Ho, J. Perkins, H.-R. Tseng, T. Yamamoto, J. F. Stoddart, J. R. Heath, *ChemPhysChem* **2002**, *3*, 519–525; e) Y. Chen, D. A. A. Ohlberg, X. Li, D. R. Stewart, R. S. Williams, J. O. Jeppesen, K. A. Nielsen, J. F. Stoddart, D. L. Olynick, E. Anderson, *Appl. Phys. Lett.* **2003**, 1610–1612; f) Y. Chen, G.-Y. Jung, D. A. A. Ohlberg, X. Li, D. R. Stewart, J. O. Jeppesen, K. A. Nielsen, J. F. Stoddart, R. S. Williams, *Nanotechnology* **2003**, *14*, 462–468; g) J. R. Heath, M. A. Ratner, *Physics Today* **2003**, May, 43–49.
- [12] a) P. R. Ashton, R. Ballardini, V. Balzani, A. Credi, R. Dress, E. Ishow, O. Kocian, J. A. Preece, N. Spencer, J. F. Stoddart, M. Venturi, S. Wenger, *Chem. Eur. J.* **2000**, *6*, 3558–3574; b) A. M. Brouwer, C. Frochet, F. G. Gatti, D. A. Leigh, L. Mottier, F. Paolucci, S. Roffia, G. W. H. Wurpel, *Science* **2001**, *291*, 2124–2128; c) F. G. Gatti, S. León, J. K. Y. Wong, G. Bottari, A. Altieri, M. A. F. Morales, S. J. Teat, C. Frochet, D. A. Leigh, A. M. Brouwer, F. Zerbetto, *Proc. Natl. Acad. Sci. USA* **2003**, *100*, 10–14.
- [13] a) J. F. Stoddart, *Chem. Aust.* **1992**, *59*, 576–577 and J. F. Stoddart, *Chem. Aust.* **1992**, *59*, 581; b) M. Gómez-López, J. A. Preece, J. F. Stoddart, *Nanotechnology* **1996**, *7*, 183–192; c) V. Balzani, M. Gómez-López, J. F. Stoddart, *Acc. Chem. Res.* **1998**, *31*, 405–414; d) V. Balzani, A. Credi, F. M. Raymo, J. F. Stoddart, *Angew. Chem.* **2000**, *112*, 3484–3530; *Angew. Chem. Int. Ed.* **2000**, *39*, 3348–3391; e) A. Harada, *Acc. Chem. Res.* **2001**, *34*, 456–464; f) C. A. Schalley, K. Beizai, F. Vögtle, *Acc. Chem. Res.* **2001**, *34*, 465–476; g) J.-P. Collin, C. Dietrich-Buchecker, P. Gaviña, M. C. Jimenez-Molero, J.-P. Sauvage, *Acc. Chem. Res.* **2001**, *34*, 477–487; h) R. Ballardini, V. Balzani, A. Credi, M. T. Gandolfi, M. Venturi, *Struct. Bonding* **2001**, *99*, 163–188; i) L. Raehm, J.-P. Sauvage, *Struct. Bonding* **2001**, *99*, 55–78; j) C. A. Stainer, S. J. Alderman, T. D. W. Claridge, H. L. Anderson, *Angew. Chem.* **2002**, *114*, 1847–1850; *Angew. Chem. Int. Ed.* **2002**, *41*, 1769–1772; k) V. Balzani, A. Credi, M. Venturi, *Chem. Eur. J.* **2002**, *8*, 5524–5532; l) H.-R. Tseng, J. F. Stoddart in *Modern Arene Chemistry* (Ed.: D. Astruc), Wiley-VCH, Weinheim, **2002**, p. 574–599; m) V. Balzani, A. Credi, M. Venturi, *Molecular Devices and Machines—A Journey into the Nano World*, Wiley-VCH, Weinheim, **2003**.
- [14] a) T. R. Kelly, H. De Silva, R. A. Silva, *Nature* **1999**, *401*, 150–152; b) N. Koumura, R. W. Zijlstra, R. A. van Delden, H. Harada, B. L. Feringa, *Nature* **1999**, *401*, 152–155; c) Y. Yokoyama, *Chem. Rev.* **2000**, *100*, 1717–1740; d) G. Berkovic, V. Krongauz, V. Weiss, *Chem. Rev.* **2000**, *100*, 1741–1754; e) B. L. Feringa, R. A. van Delden, N. Koumura, E. M. Geertsema, *Chem. Rev.* **2000**, *100*, 1789–1816; f) T. R. Kelly, *Acc. Chem. Res.* **2001**, *34*, 514–522; g) S. Shinkai, M. Ikeda, A. Sugasaki, M. Takeuchi, *Acc. Chem. Res.* **2001**, *34*, 494–503.
- [15] a) C. P. Collier, E. W. Wong, M. Belohradsky, F. M. Raymo, T. Shimizu, J. F. Stoddart, P. J. Kuekes, R. S. Williams, J. R. Heath, *Science* **1999**, *285*, 391–394; b) E. W. Wong, C. P. Collier, M. Belohradsky, F. M. Raymo, J. F. Stoddart, J. R. Heath, *J. Am. Chem. Soc.* **2000**, *122*, 5831–5840; c) R. F. Service, *Science* **2001**, *291*, 426–427; d) R. F. Service, *Science* **2001**, *294*, 2442–2443; e) M. Jacoby, *Chem. Eng. News* **2002**, Sept. 30, 38–43.
- [16] J. O. Jeppesen, J. Perkins, J. Becher, J. F. Stoddart, *Angew. Chem.* **2001**, *113*, 1256–1261; *Angew. Chem. Int. Ed.* **2001**, *40*, 1216–1221.
- [17] M. Asakawa, W. Dehaen, G. L'abbé, S. Menzer, J. Nouwen, F. M. Raymo, J. F. Stoddart, D. J. Williams, *J. Org. Chem.* **1996**, *61*, 9591–9595.
- [18] For reviews on CT and hydrogen bonding interactions, which are also a source of stabilization at these recognition sites, see: a) D. Philp, J. F. Stoddart, *Angew. Chem.* **1996**, *108*, 1242–1286; *Angew.*

- Chem. Int. Ed. Engl.* **1996**, *35*, 1154–1196; b) S. J. Rowan, S. J. Cantrell, G. R. L. Cousins, J. K. M. Sanders, J. F. Stoddart, *Angew. Chem.* **2002**, *114*, 938–993. *Angew. Chem. Int. Ed.* **2002**, *41*, 898–952. For accounts and reviews on [$\pi\cdots\pi$] stacking interactions, see: c) C. A. Hunter, J. K. M. Sanders, *J. Am. Chem. Soc.* **1990**, *112*, 5525–5534; d) M. H. Schwartz, *J. Inclusion Phenom.* **1990**, *9*, 1–35; e) J. H. Williams, *Acc. Chem. Res.* **1993**, *26*, 539–598; f) C. A. Hunter, *Angew. Chem.* **1993**, *105*, 1653–1655; *Angew. Chem. Int. Ed. Engl.* **1993**, *32*, 1584–1586; g) C. A. Hunter, *J. Mol. Biol.* **1993**, *230*, 1025–1054; h) T. Dahl, *Acta. Chem. Scand.* **1994**, *48*, 95–116; i) F. Cozzi, J. S. Siegel, *Pure Appl. Chem.* **1995**, *67*, 683–689; j) C. G. Claessens, J. F. Stoddart, *J. Phys. Org. Chem.* **1997**, *10*, 254–272; k) G. Chessari, C. A. Hunter, C. M. R. Low, M. J. Packer, J. G. Vinter, C. Zonta, *Chem. Eur. J.* **2002**, *8*, 2860–2867.
- [19] J. O. Jeppesen, K. A. Nielsen, J. Perkins, S. A. Vignon, A. Di Fabio, R. Ballardini, M. T. Gandolfi, M. Venturi, V. Balzani, J. Becher, J. F. Stoddart, *Chem. Eur. J.* **2003**, *9*, 2982–3007.
- [20] P. R. Ashton, V. Balzani, J. Becher, A. Credi, M. C. T. Fyfe, G. Matternsteig, S. Menzer, M. B. Nielsen, F. M. Raymo, J. F. Stoddart, M. Venturi, D. J. Williams, *J. Am. Chem. Soc.* **1999**, *121*, 3951–3957.
- [21] a) P. R. Ashton, R. Ballardini, V. Balzani, A. Credi, M. T. Gandolfi, D. J. F. Marquis, L. Pérez-García, L. Prodi, J. F. Stoddart, M. Venturi, A. J. P. White, D. J. Williams, *J. Am. Chem. Soc.* **1995**, *117*, 11171–11197; b) R. Castro, K. R. Nixon, J. D. Evenseck, A. E. Kaifer, *J. Org. Chem.* **1996**, *61*, 7298–7303.
- [22] a) M. Asakawa, P. R. Ashton, V. Balzani, A. Credi, C. Hamers, G. Matternsteig, M. Montalti, A. N. Shipway, N. Spencer, J. F. Stoddart, M. S. Tolley, M. Venturi, A. J. P. White, D. J. Williams, *Angew. Chem.* **1998**, *110*, 357–361; *Angew. Chem. Int. Ed.* **1998**, *37*, 333–337; b) V. Balzani, A. Credi, G. Matternsteig, O. A. Matthews, F. M. Raymo, J. F. Stoddart, M. Venturi, A. J. P. White, D. J. Williams, *J. Org. Chem.* **2000**, *65*, 1924–1936; c) M. Asakawa, M. Higuchi, G. Matternsteig, T. Nakamura, A. R. Pease, F. M. Raymo, T. Shimizu, J. F. Stoddart, *Adv. Mater.* **2000**, *12*, 1099–1102.
- [23] H.-R. Tseng, S. A. Vignon, J. F. Stoddart, *Angew. Chem.* **2003**, *115*, 1529–1533; *Angew. Chem. Int. Ed.* **2003**, *42*, 1491–1495.
- [24] P.-L. Anelli, P. R. Ashton, N. Spencer, A. M. Z. Slawin, J. F. Stoddart, D. J. Williams, *Angew. Chem.* **1991**, *103*, 1052–1055; *Angew. Chem. Int. Ed. Engl.* **1991**, *30*, 1036–1039.
- [25] P. R. Ashton, R. Ballardini, V. Balzani, S. E. Boyd, A. Credi, M. T. Gandolfi, M. Gómez-López, S. Iqbal, D. Philp, J. A. Precece, L. Prodi, H. G. Ricketts, J. F. Stoddart, M. S. Tolley, M. Venturi, A. J. P. White, D. J. Williams, *Chem. Eur. J.* **1997**, *3*, 152–170.
- [26] J. O. Jeppesen, J. Perkins, J. Becher, J. F. Stoddart, *Org. Lett.* **2000**, *2*, 3547–3550.
- [27] P. R. Ashton, R. Ballardini, V. Balzani, M. Belohradsky, M. T. Gandolfi, D. Philp, L. Prodi, F. M. Raymo, M. V. Reddington, N. Spencer, J. F. Stoddart, M. Venturi, D. J. Williams, *J. Am. Chem. Soc.* **1996**, *118*, 4931–4951.
- [28] R. Andreu, J. Garín, J. Orduna, M. Saviron, J. Cousseau, A. Gorgues, V. Morisson, T. Ozdryn, J. Becher, R. P. Clausen, M. R. Bryce, P. J. Skabara, W. Dehaen, *Tetrahedron Lett.* **1994**, *35*, 9243–9246.
- [29] J. G. Hansen, K. S. Bang, N. Thorup, J. Becher, *Eur. J. Org. Chem.* **2000**, *11*, 2135–2144.
- [30] P. R. Ashton, G. R. Brown, N. S. Isaacs, D. Giuffrida, F. H. Kohnke, J. P. Mathias, A. M. Z. Slawin, D. R. Smith, J. F. Stoddart, D. J. Williams, *J. Am. Chem. Soc.* **1992**, *114*, 6330–6353.
- [31] Y.-K. Han, A. Reiser, *Macromolecules* **1998**, *31*, 8789–8793.
- [32] In the case of the [2]rotaxane **5-4PF₆**, it has been demonstrated that no intermolecular aggregation occurs in the concentration range from 4.8×10^{-6} M up to 4.8×10^{-4} M in MeCN. Starting from a solution of **5-4PF₆** with the higher concentration and diluting it stepwise down to the lower concentration, no deviation from linear Lambert–Beer behavior was observed at five different wavelengths, namely 337, 361, 470, 700, and 845 nm.
- [33] P.-L. Anelli, P. R. Ashton, R. Ballardini, V. Balzani, M. Delgado, M. T. Gandolfi, T. T. Goodnow, A. E. Kaifer, D. Philp, M. Pietraszkiewicz, L. Prodi, M. V. Reddington, A. M. Z. Slawin, N. Spencer, J. F. Stoddart, C. Vicent, D. J. Williams, *J. Am. Chem. Soc.* **1992**, *114*, 193–218.
- [34] I. B. Berlman, *Handbook of Fluorescence Spectra of Aromatic Molecules*, Academic Press, London, **1971**.
- [35] a) P. R. Ashton, R. Ballardini, V. Balzani, M. Belohradsky, M. T. Gandolfi, D. Philp, L. Prodi, F. M. Raymo, M. V. Reddington, N. Spencer, J. F. Stoddart, M. Venturi, D. J. Williams, *J. Am. Chem. Soc.* **1996**, *118*, 4931–4951; b) R. Ballardini, V. Balzani, W. Dehaen, A. E. Dell'Erba, F. M. Raymo, J. F. Stoddart, M. Venturi, *Eur. J. Org. Chem.* **2000**, 591–602.
- [36] A. Gilbert, J. Baggott, *Essentials of Molecular Photochemistry*, Blackwell Scientific Publications, Oxford, **1991**.
- [37] a) K. B. Simonsen, J. Becher, *Synlett* **1997**, 1211–1220; b) M. R. Bryce, *J. Mater. Chem.* **2000**, *10*, 590–598; c) J. O. Jeppesen, J. Becher, *Eur. J. Org. Chem.* **2003**, 3245–3266.
- [38] A. Zweig, A. H. Maurer, B. G. Roberts, *J. Org. Chem.* **1967**, *32*, 1322–1329.
- [39] E. A. Smith, R. R. Lilienthal, R. J. Fonseca, D. K. Smith, *Anal. Chem.* **1994**, *66*, 3013–3020.
- [40] The DNP moiety encircled by CBPQT⁴⁺ is oxidized at +1.55 V; see ref. [22a].
- [41] M. Asakawa, P. R. Ashton, V. Balzani, A. Credi, G. Matternsteig, O. A. Matthews, M. Montalti, N. Spencer, J. F. Stoddart, M. Venturi, *Chem. Eur. J.* **1997**, *3*, 1992–1996.
- [42] a) E. Córdova, R. A. Bissell, N. Spencer, P. R. Ashton, J. F. Stoddart, A. E. Kaifer, *J. Org. Chem.* **1993**, *58*, 6550–6552; b) E. Córdova, R. A. Bissell, A. E. Kaifer, *J. Org. Chem.* **1995**, *60*, 1033–1038.
- [43] The peak asymmetry (Figure 7) associated with the second reduction process for the [2]rotaxanes **1⁴⁺** and **3⁴⁺** disappears when the differential pulse voltammograms are performed under standard conditions ($v = 20 \text{ mV s}^{-1}$, pulse height = 75 mV). This observation suggests that a very small amount of another electroactive species might be present in the MeCN solution at room temperature. This species could be a trace of impurity or a minor quantity of the other translational isomer where the CBPQT⁴⁺ ring is located on the DNP moiety.
- [44] a) T. Pascher, J. P. Chesick, J. R. Winkler, H. B. Gray, *Science* **1996**, *271*, 1558–1560; b) E. Chen, P. Wittung-Stafshede, D. S. Kliger, *J. Am. Chem. Soc.* **1999**, *121*, 3811–3817; c) J. C. Lee, H. B. Gray, J. R. Winkler, *Proc. Natl. Acad. Sci. USA* **2001**, *98*, 7760–7764; d) G. P. Dado, S. H. Gellman, *J. Am. Chem. Soc.* **1993**, *115*, 12609–12610.
- [45] a) S. Hünig, G. Kiebllich, H. Quast, D. Scheutzw, *Liebigs Ann. Chem.* **1973**, 310–323; b) G. Schukat, E. Fanghänel, *J. Prakt. Chem.* **1985**, *327*, 767–774; c) A. Credi, M. Montalti, V. Balzani, S. J. Langford, F. M. Raymo, J. F. Stoddart, *New J. Chem.* **1998**, *22*, 1061–1065.
- [46] This oxidant was chosen for three reasons—1) it has a high enough oxidative potential (0.7 V vs ferrocene) to oxidize the TTF unit completely to TTF²⁺, 2) the reduced form will give only two signals in the ¹H NMR spectrum and will not interfere with the interpretation of the data, and 3) the solubilities of both the oxidant and its reduced form are as good in the same solvents as the rotaxanes of interest. For details, see: a) N. G. Connelly, W. E. Geiger, *Chem. Rev.* **1996**, *96*, 877–910; b) E. Steckhan, *Top. Curr. Chem.* **1987**, *142*, 1–69.
- [47] T. J. Huang, H.-R. Tseng, L. Sha, W. Lu, B. Brough, B. Yu, P. C. Cel-estre, P. J. Chang, J. F. Stoddart, C.-M. Ho, submitted.
- [48] D. D. Perrin, W. L. F. Armarego, *Purification of Laboratory Chemicals*, Pergamon Press, New York, **1998**.
- [49] R. Ballardini, V. Balzani, M. T. Gandolfi, R. E. Gillard, J. F. Stoddart, E. Tabellini, *Chem. Eur. J.* **1998**, *4*, 449–459.
- [50] S. F. Nelsen, L.-J. Chen, M. T. Ramm, G. T. Voy, D. R. Powell, M. A. Aceola, T. R. Seehafer, J. J. Sabelko, J. R. Pladziewicz, *J. Org. Chem.* **1996**, *61*, 1405–1412.
- [51] I. Noviandri, K. N. Brown, D. S. Fleming, P. T. Gulyas, P. A. Lay, A. F. Masters, L. Phillips, *J. Phys. Chem. B* **1999**, *103*, 6713–6722.
- [52] J. B. Flanagan, S. Margel, A. J. Bard, F. C. Anson, *J. Am. Chem. Soc.* **1978**, *100*, 4248–4253.
- [53] E. P. Parry, R. A. Osteryoung, *Anal. Chem.* **1965**, *37*, 1634–1637.

Received: June 4, 2003
Revised: August 21, 2003 [F5204]